MICROCOPY RESOLUTION TEST CHART
NS-1963-A

FINAL REPORT

AD-A188 981

PROCESSING, MICROSTRUCTURE, AND MECHANICAL PROPERTIES
OF SILICON CARBIDE PARTICULATE REINFORCED ALUMINUM ALLOYS

CONTRACT NUMBER· DAAG29-84-K-0174

Chikara Fujiwara
Joseph Blucher
James A. Cornie

MASSACHUSETTS INSTITUTE OF TECHNOLOGY
77 Massachusetts Avenue, Cambridge, Mass. 02139

Period of performance:

September 10, 1984 to October 31, 1987

DTIC
ELECTE
FEB 0 2 1988
S
D
H

88 1 27 089

REPORT DOCUMENTATION PAGE

Form Approved
OMB No. 0704-0188

1a. REPORT SECURITY CLASSIFICATION	1b. RESTRICTIVE MARKINGS
Unclassified	
2a. SECURITY CLASSIFICATION AUTHORITY	3. DISTRIBUTION/AVAILABILITY OF REPORT
2b. DECLASSIFICATION/DOWNGRADING SCHEDULE	Approved for public release. Distribution unlimited.
4. PERFORMING ORGANIZATION REPORT NUMBER(S)	5. MONITORING ORGANIZATION REPORT NUMBER(S)
	ARO 21530.1-MS

6a. NAME OF PERFORMING ORGANIZATION	6b. OFFICE SYMBOL (If applicable)	7a. NAME OF MONITORING ORGANIZATION
Massachusetts Institute of Technology		U. S. Army Research Office
6c. ADDRESS (City, State, and ZIP Code)		7b. ADDRESS (City, State, and ZIP Code)
77 Massachusetts Avenue Cambridge, MA 02139		P. O. Box 12211 Research Triangle Park 27709-221

8a. NAME OF FUNDING/SPONSORING ORGANIZATION Army Research Office, Materials Science Div.	8b. OFFICE SYMBOL (If applicable)	9. PROCUREMENT INSTRUMENT IDENTIFICATION NUMBER
		DAAG29-84-K-0174

8c. ADDRESS (City, State, and ZIP Code)	10. SOURCE OF FUNDING NUMBERS			
4300 South Main Boulevard Research Triangle Park, NC 27709-1211	PROGRAM ELEMENT NO.	PROJECT NO.	TASK NO.	WORK UNIT ACCESSION NO.

11. TITLE (Include Security Classification)

Processing, Microstructure, and Mechanical Properties of Silicon Carbide Particulate Reinforced Aluminum Alloys

12. PERSONAL AUTHOR(S)

Chikara Fujiwara, Joseph Blucher, James A. Cornie

13a. TYPE OF REPORT	13b. TIME COVERED	14. DATE OF REPORT (Year, Month, Day)	15. PAGE COUNT
Final	FROM 9/10/84 TO 10/31/87	1988 January 14	66

16. SUPPLEMENTARY NOTATION The view, opinions and/or findings contained in this report are those of the author(s) and should not be construed as an official Department of the Army position, policy, or decision, unless so designated by other documentation.

17. COSATI CODES			18. SUBJECT TERMS (Continue on reverse if necessary and identify by block number)
FIELD	GROUP	SUB-GROUP	Silicon carbide, composites, ball milling, microstructure

19. ABSTRACT (Continue on reverse if necessary and identify by block number)

SiC particulate reinforced Al-2%Mg composites were produced at volume fractions of inert atmosphere ball milling followed by Hot Isostatic Pressing extrusion. The SiC particulate sizes evaluated were 5 microns, 1 micron, and .2 microns. The processing sequences were carefully controlled to minimize oxygen contamination. The resulting microstructures of the as-extruded materials showed a very uniform distribution of particulates within the matrix.

Ultimate strength, 0.2% yield strength, and modulus of elasticity increased with decreasing SiC particulate size; 1 micron SiC-Al matrix showed the highest elongation.

Fractures originated at inclusions rich in iron, chromium, and nickel. These contaminants seemed to come from the mill chamber and/or the hardened steel balls during ball milling.

20. DISTRIBUTION/AVAILABILITY OF ABSTRACT	21. ABSTRACT SECURITY CLASSIFICATION
☐ UNCLASSIFIED/UNLIMITED ☒ SAME AS RPT. ☐ DTIC USERS	UNCLASSIFIED
22a. NAME OF RESPONSIBLE INDIVIDUAL	22b. TELEPHONE (Include Area Code)	22c. OFFICE SYMBOL
George Prendergast	(617) 253-0308	

DD Form 1473, JUN 86   Previous editions are obsolete.   SECURITY CLASSIFICATION OF THIS PAGE

TABLE OF CONTENTS

QUALITY INSPECTED 2

Accession For	
NTIS GRA&I	☑
DTIC TAB	☐
Unannounced	☐
Justification	
By	
Distribution/	
Availability Codes	

Dist	Avail and/or Special
A-1	

PROCESSING, MICROSTRUCTURE, AND MECHANICAL PROPERTIES
OF SILICON CARBIDE PARTICULATE REINFORCED ALUMINUM ALLOYS

ABSTRACT

SiC particulate reinforced Al-2%Mg composites were produced at volume fractions 0.1, 0.2, and 0.3 by inert atmosphere ball milling followed by hot isostatic pressing (HIP) consolidation and extrusion. The SiC particulate sizes evaluated were 5 microns, 1 micron, and 0.2 microns. The processing sequences were carefully controlled to minimize oxygen contamination. The resulting microstructures of the as-extruded materials showed a very uniform distribution of particulates within the matrix.

Ultimate strength, 0.2% yield strength, and modulus of elasticity increased with decreasing SiC particulate size; 1 micron SiC-Al matrix showed the highest elongation.

Fractures originated at inclusions rich in iron, chromium, and nickel. These contaminants seemed to come from the mill chamber and/or the hardened steel balls during ball milling.

INTRODUCTION

It has been demonstrated that the dispersion of SiC particulates in an aluminum matrix is an effective way to increase significantly both the tensile strength and the stiffness of aluminum alloys. Unfortunately, the fracture toughness of these SiC/ Aluminum composites decreases with increasing volume percent of the SiC particulates and in general has such low values that the application in these composites is limited.

It is known that microstructure has important effects on the mechanical properties of alloys. For example, the yield strength, fracture strength, and the strain at failure of low carbon steels increase with decreasing grain size. Consequently, it is expected that the mechanical properties of particlulate reinforced aluminum alloys will improve when their microstructure is refined.

Presently, the metal matrix composite industry is working mostly with easily available 2-10μm grinding grade SiC and -325 mesh aluminum powder, consolidating their large components with conventional powder metallurgy technology. In all probability, the resulting rather inhomogeneous and coarse microstructure contributes to the low fracture toughness of these composites.

There are limited amounts of systematic studies published on the relation of mechanical properties to microstructure, therefore this research program is aimed at filling that gap; namely to investigate how the microstructure of particulate reinforced aluminum matrix composite influences the mechanical properties of the composites.

It is expected that, apart from the processing technology, the particulate size has a major influence on the microstructure: finer particulates yielding finer microstructures.

Therefore the thrust of the program will be two fold:

A.   To develop a process to produce SiC particulate (such as 1 micron and 0.2 micron particulate) reinforced aluminum alloy composites with very uniform particulate distribution.

B.   To investigate the effect of the SiC particulate size on the mechanical properties of composites, with special attention to the effect of ultrafine particulates.

EXPERIMENTAL PROCEDURE

A . MATERIALS:

a.) Matrix:

Al-2Mg was selected for the matrix. This alloy in solution strengthened, has sufficiently high recrystallization temperature to preserve the microstructure and was thoroughly investigated in the pa:· with and without Al_2O_3 dispersion strengthening.

The master alloy was purchased from Reynolds Aluminum. The powders were manufactured from the master remelt ingots via inert gas atomization at Valimet Co. The chemical analysis of the master alloy and the atomized powder is given in Table I. Loss of magnesium during atomization was negligible. Figure 1 shows SEM photograph of atomized - 320 mesh powder.

b.) SiC Particulates

Four sizes of SiC particulates were selected as reinforcing materials. Three sizes were available semi-commercially from Norton Company. Their nominal particulate sizes were 5 microns, 1 micron and 0.2 micron. The fourth size was produced at M.I.T. with a proprietary laser induced chemical vapor precipitation process. The nominal particle size of this powder is 200 angstroms.

B. PROCESS TO MIX THE COMPONENTS

To obtain a homogeneous distribution of the particulates in the matrix the interparticulate spacing has to be controlled.

The interparticle spacing of reinforcing particulates in a metal matrix is a function of the particle size and the volume fraction. The spacing decreases with decreasing particle size and with increasing volume fraction. For example, the calculated interparticle spacing is 0.3 micron for a composite with particle size of 0.2 micron and a volume fraction of 30%. Obviously, the as atomized — 325 mesh powder is far too coarse to allow such a small interparticle spacing, therefore the as atomized powder has to be comminuted to submicron sizes.

As a proven technology to comminute metal powders to submicron sizes, wet attrition was tried first. In the experiment 280 grams of -320 mesh Al-2% Mg powder was attrited. The attrition was accomplished in a 1 gallon Szegvari attritor in which the powder was charged with 3 liters of ethyl alcohol and 11 kilograms of 3 mm hardened steel balls. The attritor operated at a rate of 120 r.p.m.. Powder samples were taken after 1, 2, 6 and 12 hours comminution. SEM

3

photographs of these samples are shown in Figure 2. The samples show that the comminuted particles have a flake like appearance with thickness less than one micron for comminution time less than one hour. As the attriting time increases, some cold welding occurs and the laminated flakes are broken to small pieces.

Although the wet attrition yielded the desired particle dimension, the process was abandoned after the first trial. With the very large fresh surfaces of the attrited powder, both oxidation and a reaction to form Al_5C_3 with the alcohol were significant.

In light of the chemical reactions during the attrition and minor but still bothersome difficulties which arose from the handling and drying of the wet metal powder, it was decided that the comminution of the metal powder and the intermixing of the SiC particulates would be attempted simultaneously with a ball mill technology resembling mechanical alloying. Mechanical alloying is a high energy, dry milling process in which the constituent powder particles are repeatedly fractured and cold welded by the continuous impacting action of steel balls to produce materials with high homogeneity.

For our work, a 17.5 cm diameter by 26 cm long ball mill was used. 4.6 kilograms of 2.5 cm diameter hardened steel balls, 4.6 kilograms of 1.9 cm diameter balls and 4.2 kilograms of 1.3 cm diameter balls were charged in the mill. The maximum operating speed of a mill is a function of the diameter. For our mill, 55 r.p.m. was determined to be suitable.

Ball milling of aluminum requires the addition of a process control agent to prevent excessive cold welding of aluminum to itself, to the ball charge, and to the mill chamber. Several agents, such as Nopcowax 22-DS, Decane, Decahydro-naphtalene, Naphtalene and Iso-Octane, were tried. Nopcowax 22-DS (C_2H_2-2 ($C_{18}H_{36}ON$)), a powdered organic wax lubricant, was chosen as the most efficient. The amount of control agent must be enough to prevent excessive welding of the aluminum, but not so much as to completely prohibit it; a dynamic balance between fracturing and welding is necessary. The optimum amount was found to be 2.5wt% of the aluminum powder charge.

In the first ball milling experiments, 280 grams of -320 mesh Al-2%Mg powder was ball milled, without SiC particulates addition. The ball milling time varied from 3 hours to 12 hours. Figure 3 shows SEM microphotographs of milled powder samples. The morphologies of ball milled aluminum powder were identical with those of the attrited aluminum powder (Figure 2); the 320 mesh Al-2% Mg powder was effectively comminuted to flakes with thickness less than one micron by ball milling.

Next, 270 grams of aluminum alloy powder and 80 grams of 2 μm SiC particulate were charged in the ball mill chamber with 7 grams of Nopcowax. The mill chamber was evacuated, backfilled with argon to 10 psi pressure and then sealed. Ball mill time varied from 1 hour to 24 hours. Figure 4 shows the microstructures and morphologies of this ball milled powder. The progress of mechanical blending is clearly illustrated here. Aluminum powders were communited

4

to flakes, the flakes were repeatedly welded and fractured, while embedding SiC particulates between them. Consequently, the dispersion of SiC particulates in an aluminum matrix became more and more uniform with the ball milling time. Since a considerably uniform dispersion was obtained after 12 hour ball milling, that time was selected for the processing of the alloys.

C. CONSOLIDATION OF THE COMPOSITE POWDERS.

Hot Isostatic Pressing followed by Extrusion was selected to consolidate the powders. The process steps to prepare the powders for the consolidation are as follows:

a.) Powder Handling

The high reactivity of the freshly comminuted powders required special attention with regard to their handling. The ball milled powder exposed to air immediately begins to burn, i.e., vigorous oxidation occurs.

In order to prevent the oxidation of the ball milled powder, all handling of the powders was done in a dry box. Following the ball milling, the sealed ball mill chamber was carried into the dry box in which the argon atmosphere was purified with a recirculating titanium getter system to less than 10^{-7}ppm oxygen. In this atmosphere the mill chamber was opened and the ball milled powder was transferred from the mill chamber into an aluminum capsule for HIP.

The capsules for HIP-ing were fabricated from tubes by welding, with dimensions of 4.8 cm inside diameter by 12 cm long. A 0.95 cm inside diameter evacuation tube was joined on one end (Figure 5). Both mild steel and 6061 Aluminum were tried as capsule material. The steel capsules cracked at the relatively low HIP temperature therefore 6061 Aluminum was used. Weldments on the capsules were Helium leak tested prior to filling them with powders.

The capsules were filled with the powder through the evacuation tube. This process was very cumbersome.

Difficulties were experienced in packing the powder in the capsule, resulting in poor packing density. This problem had a rather negative effect on the yield of usable test specimens. At the end of the program, some powder was cold compacted before encapsulation for HIP. With these billets, a much higher yield of usable specimens are expected. Unfortunately, due to the termination of the program and recurring failures in the HIP equipment, these billets are not HIP-ed yet at this time.

b) Dewaxing

To eliminate contamination from the wax, dewaxing of the blended composite powder was performed before HIP-ing. The filled capsules were connected to a vacuum system of 10^{-6} mm Hg ultimate pressure and heated to 250° C and held for one hour, then to 350° C for twenty four

hours. Since aluminum and carbon react to form aluminum carbide (Al_4C_3) above 400° C (24), the maximum dewaxing temperatures were chosen below that temperature.

When the dewaxing was finished, the evacuation tubes were sealed by cold welding followed by arc welding.

c.) HIP-ing and Extrusion

The capsules were HIP-ed at 580° C for 2 hours at Industrial Materials Technology, Inc.. The HIP pressure was 103 MPa. Figure 6 shows the record chart. Due to the poor packing of ball milled powder, the HIP-ed capsules were highly collapsed in volume and irregularly deformed as seen in Figure 5.

To make possible the extrusion of irregular shapes obtained by HIP with an approximately 35 to 1 extrusion ratio, the HIP-ed shapes were enclosed in 6061 aluminum sleeves. The bars were extruded at 475° C . As it was expected, the irregular shape of the HIP-ed form was maintained throughout the extrusion, severely limiting the number of specimens one could machine out from them.

EVALUATION OF THE COMPOSITES

At the end there were seven alloys which could be evaluated for structure and mechanical properties. This was less than originally planned. One composition of the 1μm and 0.2μm alloys were lost during HIP. The two alloys with the ultrafine powder were encapsulated but not HIP-ed because of repeated failure of the HIP equipment. A matrix of the investigated alloys is shown in Table II.

A. MECHANICAL TESTING

Tensile test of the extruded composites were performed at room temperature. For each composite three specimens were tested. The specimen configurations are shown in Figure 7. Due to the irregular and small collection of the extruded composites, both round and rectangular specimens had to be used.

The tests were performed on an Instron tensile testing machine at a crosshead speed of 0.05 cm (0.02 inch) per minute. The stress strain curves were recorded by using an extensometer. From these curves, the 0.2% yield strength, percent elongation, and modulus of elasticity were determined.

Stress versus strain curves for SiC/Al composites containing 10 and 30 v/o 5 μm, 1μm, and 0.2 μm reinforcement are shown in Figures 8 and 9 respectively.

Figures 10 to 12 are graphs of ultimate strength, 0.2% yield strength, modulus of elasticity

and percent elongation versus the logarithm of SiC particle diameter. Both the ultimate strength and 0.2% yield strength increased with decreasing SiC particle diameter. The increment was larger for 30 v/o SiCp/Al composites. The modulus of elasticity of the alloy increased with decreasing SiC particle size. Percent elongation showed a peak at around $1.0\mu m$ reinforcement size.

Figure 13 shows SEM fractographs of tensile tested composites. The fracture surface consists of fine, equiaxed ductile dimples of uniform size. These dimples were present in spite of the low elongation of the alloys.

Figures 14 and 15 show fractures originating from inclusion. EDAX analysis showed the inclusions rich in iron, chromium and nickel. It seems conceivable that small fragments from the ball mill chamber reacted with the aluminum to form iron, chromium and nickel rich intermetallics, and fragments from the hardened steel balls to form iron rich intermetallics.

Figure 16 shows SEM fractographs of a tensile tested specimen of the as-HIPed C-2 composites. Aluminum flakes were, as opposed to dimples, observed on the fracture surface. The ultimate strengths of the as-HIPed C-2 composite were 225 and 130 MPa while the ultimate strengths of the extruded C-2 composites were 510, 490 and 490 MPa, showing that extrusion is an essential step for the consolidation of the composites.

B. CHEMICAL ANALYSIS TO DETERMINE CONTAMINATION OF THE ALLOYS

We were concerned with two types of contamination: elements from the ball milling chamber, and ball and oxygen pick-up. Samples of the C-1 and C-6 alloy were chemically analyzed for contaminants expected from the ball milling procedure. Table III summarizes the chemistry of the alloys. When these composition are compared to the atomized Al-2Mg powder it is evident that contamination occurred from the abrasion of the chamber wall and the balls. It appears that the abrasion rate, and consequently the contamination rate, is related to the size of the SiC particulates. The coarse SiC is more abrading than the fine powder; the C-1, 5 micron SiC/Al-2%Mg composite, had more contaminants than the C-5, 0.2 micron SiC/Al-2%Mg composite.

This type of contamination could be reduced by changing the surface composition of the chamber and balls.

The as-HIPed composites were analysed for oxygen contamination. The results are given in Table IV. Despite careful handling of the powder, oxidation occurred to some extent. The major source of the oxygen pick-up is thought to be the dewaxing operation. However, in spite of the contamination the oxygen level is still substantially lower than it would be if the powders were attrited and mixed in air.

C. ANALYSIS OF THE STRUCTURE

HIP-ed and extruded composites were investigated by optical microscopy and scanning and transmission electron microscopy.

a.) Optical Microscopy

Keller's reagent was used to etch the specimens. Figure 17 shows the microstructures of the as HIP-ed composites. Even though some SiC particulate free regions were observed, the SiC particulates were satisfactorily dispersed.

Figure 18 shows microstructures of extruded composites. Clearly the uniformity of dispersion was improved by extrusion. The lamellar constituent was not observed; all white regions free from SiC particles had disappeared.

b.) Scanning and Transmission Electron Microscopy

Microstructural features studied included the SiC particle size and distribution, and the composition of SiC-Al interface. An attempt has been made to determine the mechanisms of composite failure, by examining the fractured SiC/Al composite specimens. Furthermore, the size and distribution of the SiC particles has been compared with that in the commmercially available composites.

D. EXPERIMENTAL PROCEDURE

SiC/Al composites with SiC particle sizes equal or greater than $1\mu m$ were examined in the unetched condition in the scanning electron microscope (SEM). The SiC/Al composites with the SiC particle size of $0.2\ \mu m$ were examined by the transmission electron microscopy (TEM). Sample preparation for TEM included electropolishing followed by ion milling. Electropolishing was carried out in a 33% solution of HNO_3 in alcohol, at -45° C and 32-34 mA. A composition of the SiC/Al interface and the second-phase particles were examined by the scanning transmission electron microscopy (STEM). Sample preparation for STEM turned out to be more elaborate than for TEM. It has been established, after sever trials, that a proper technique includes a thinning of TEM disks to approximately $10\ \mu m$ by electropolishing or alternatively, by mechanical dimpling and followed by ion milling. Tensile fracture surfaces were prepared for the SEM examination by attaching two fracture ends with adhesive and metallographic polishing. These specimens were examined in the SEM in the unetched condition.

8

RESULTS AND DISCUSSION

a.) SiC Particle Size and Distribution

Composites containing 1 and 5μm Sic particles were examined by the SEM. As shown in Figures 19 to 21, the SiC particle size in the 5-10, 5-20 and 5-30 composites is quite uniform.

There are two features in Figure 20 which are worth noting, namely, some SiC particle appear to pre-crack during powder processing (location A); furthermore, "pull-out" may be observed in he aluminum matrix (location B) and they most probably correspond to poor local bonding of aluminum powders due to their surface oxide film. Both the pre-cracked SiC particles and surface oxide film may serve as possible fracture nucleation centers.

With 1 μm SiC particle size the distribution remains uniform. This is shown in Figures 22 and 23 for the 1-10 and 1-30 composites, respectively.

Figure 23 is a TEM micrograph of the 0.2-10 composite consolidated by the HIP. SiC particles appear to be concentrated along the prior particle boundaries and their distribution reflects directly the condition of the powder processing. Subsequent extrusion did not randomize the SiC particle distribution. As shown in Figure 25, SiC particles appear to be clustered along the cell boundaries, approximately 1 μm in size.

b) Composition of the Second-Phase Particles.

Figure 26 is a low magnification TEM micrograph of the 1-10 composite. It shows the average grain size, which is of the order of 1 μm and smaller, and the distribution of the second-phase particles in the aluminum matrix. HIP and extrusion distributed second-phase particles preferentially along the grain boundaries. Their size ranges for few 10 to 100 μm and their morphology is distinctly different from that of the SiC particles.

STEM analysis showed that the majority of the second-phase particles are rich in magnesium and oxygen. They are formed, presumably, through the reduction of Al_2O_3 by magnesium during high temperature processing and yielding MgO, an oxide with a lower free energy. Such a magnesium and oxygen rich particle is shown in the upper left corner of Figure 9 and its composition is given in Figure 27.

X-ray microanalysis of the second phase particles revealed, in addition to magnesium and oxygen rich particles, several particles containing iron and chromium. They formed, most likely, during the powder processing (i.e., from contamination during ball milling). The size and morphology of the iron and chromium rich particles is comparable to that of the MgO particles.

9

c) Compositional Variation at the SiC/Al Interface

The composition and the structure of the SiC/Al interface is of considerable interest in developing SiC/Al composites with sufficiently high fracture toughness. It has been established that, depending on the nature of the interface, deformation and fracture processes may proceed either through void initiation at the interface or, alternatively, through interface decohesion involving the thin oxide layer.

The compositional variation at the SiC/Al interface has been analyzed by STEM in two randomly chosen SiC particles in the 0.2-10 composite. Such an interface is shown in Figure 28 with the location of the measurement indicated. There is no evidence of discrete precipitates along the SiC/Al boundary. The results of the x-ray microanalysis across the SiC/Al interface are shown in Figure 29. Spectra were acquired at points 25 and 50 μm apart along the trace running normal to the interface. The x-ray spectrum from each point was processed and the concentration of magnesium was expressed as the ration of magnesium and aluminum integrated peak intensities. Results in Figure 29 indicate only slight enrichment of magnesium at the SiC/Al interface. This is in contrast to significant enrichment of magnesium along the precipitate free SiC/Al interface in a study reported by Nutt and Carpenter [see Figure 4, p. 173, Materials Science and Engineering, 75 (1985)]. In their work, composites (i.e., aluminum reinforced with SiC whiskers) were fabricated by powder metallurgy process which involved consolidiation by compression above the alloy solidus temperature, followed by hot extrusion. Consolidation of P/M composites above the alloy solidus temperature presumably allows migration and coalescence of magnesium oxide particles, thereby reducing interfacial energies. This process enhances interface decohesion. The composites in the present study have been HIP-ed in the solid state and this may explain considerably smaller enrichment of magnesium along the precipitate free SiC/Al interface.

d) Deformation and Fracture Process

Figures 30 and 31 are the SEM micrographs of the 5-10 and 5-30 tensile tested composites, respectively. They show areas next to the fracture surface, which is indicated as FS, (top) and areas at some distance beneath the fracture surface (bottom). Highly deformed regions beneath bulk tensile fracture surfaces are of particular interest as they reveal possible fracture nucleation centers as well as the sites of stress concentration where intense plastic flow has occurred. Fracture in 5-10 composites appears to initiate at sites such as location A in Figure 30, and it may be associated with poor bonding of aluminum powders due to their surface oxide film. This view is enhance by the observations of "pull-outs" in the undeformed 5-10 composite, such as location B in Figure 19. Observations in Figures 30 and 31 (bottom) suggest that damage at sites, presumable associated with poor bonding of aluminum powders, precedes the decohesion or void formation at the SiC/Al interface and as such it may initiate the premature fracture process in the composite, and thus lower ductility and fracture toughness.

e) Comparison of the SiC distribution with Commercial Si/C Composites.

SiC particle distribution in 5-30 composite has been compared with that of the commercially available SiC/Al composites by taking randomly several low magnification SEM micrographs. Such areas are shown in Figures 32 and 33 for a commercial SiC/Al composite. Consolidation of the commercial composite was carried out by vacuum hot pressing (Figure 32) and hot isostatic pressing(Figure 34). It resulted, in both cases, in a not-uniform distribution of the SiC particles in the aluminum matrix. In contrast, the 5-30 composite in the present study which was consolidated by hit isostatic pressing followed by extrusion showed an essentially uniform SiC distribution (see Figure 34).

CONCLUSIONS

The following conclusions can be drawn from the accomplished work:

1.) Ball milling-mixing is a suitable technological step to produce SiC reinforced aluminum metal matrix composites. The distribution of the SiC particulates in the matrix is considerably more uniform in the composites produced with the ball milling technology than in composites commercially available.

2.) Due to the closed system powder handling, oxygen levels in the composites produced in this program are significantly lower than would be expected if the attrition mixing occurred in air.

3.) Contamination from the components of the ball mill is noticeable; however, it could be reduced through coating the milling chamber and the balls.

4.) Extrusion is an essential step for the consolidation of the powders. HIP alone does not break down Al_2O_3 films on the Al particulate surfaces, resulting in poor cohesion between particles.

5.) Ultimate strength, yield strength and modulus of elasticity increase with decreasing particle size.

6.) In the range of three particle sizes (5μm, 1μm, and 0.2μm) elongation appears to peak at 1μm particle size.

7.) The low initial packing density of canned powder resulted in an insufficient number of specimens for mechanical testing. Moreover, with the uneven cross-section of the HIP-ed specimens, the amount of hotwork introduced into the materials during extrusion was varied significantly. Consequently, the testing results can be regarded only as tendencies.

8.) Metallic contamination forming inclusions appears to contribute to failure initiation.

12

SUGGESTIONS FOR FURTHER WORK

- The test matrix should be extended by completing composites with the ultrafine SiC and repeating some of the tested composites. Presently, four alloys are encapsulated and will be HIP-ed upon availability of HIP equipment.

- In addition to the confirmation and extension of the existing room temperature mechanical test data, high temperature properties of these composites should be investigated.

- Through changing the processing steps, oxygen and metallic contamination should be reduced to increase strength and ductility rates.

13

LIST OF TABLES

LIST OF FIGURES

15

TABLE I

Chemical Compositions (wt%)

Master alloy

Al	Mg	Fe	Ni	Cr	Si	Cu	Mn	Zn	Ti
Bal.	2.31	0.008	<0.002	<0.002	0.012	<0.002	< 0.002	0.005	<0.002

Atomized powder

Al	Mg	Fe	Ni	Cr	Si	Cu	Mn	Zn	Ti
Bal.	2.33	0.018	0.008	<0.001	0.019	0.019	0.005	0.002	<0.001

TABLE II

Test Matrix

Composite	SiC particulate size	Volume fraction
C-1	5 microns	10 %
C-2	5 microns	20 %
C-3	5 microns	30 %
C-4	1 micron	10 %
C-5	1 micron	30 %
C-6	0.2 micron	10 %
C-7	0.2 micron	30 %

TABLE III

Chemistry of Ball Milled Composites

Composite	Composition (wt %)		
	Fe	Cr	Ni
C-1	1.86	0.257	0.038
C-6	0. 49	0.075	0.011

TABLE IV

Oxygen Contents of as HIPed Composites

Composite	Oxygen (wt %)
C-1	1.58
C-2	1.21
C-3	0.83
C-4	1.17
C-5	1.89
C-6	1.61
C-7	2.21
Atomized Al-2%Mg Powder (-325 mesh)	0.75
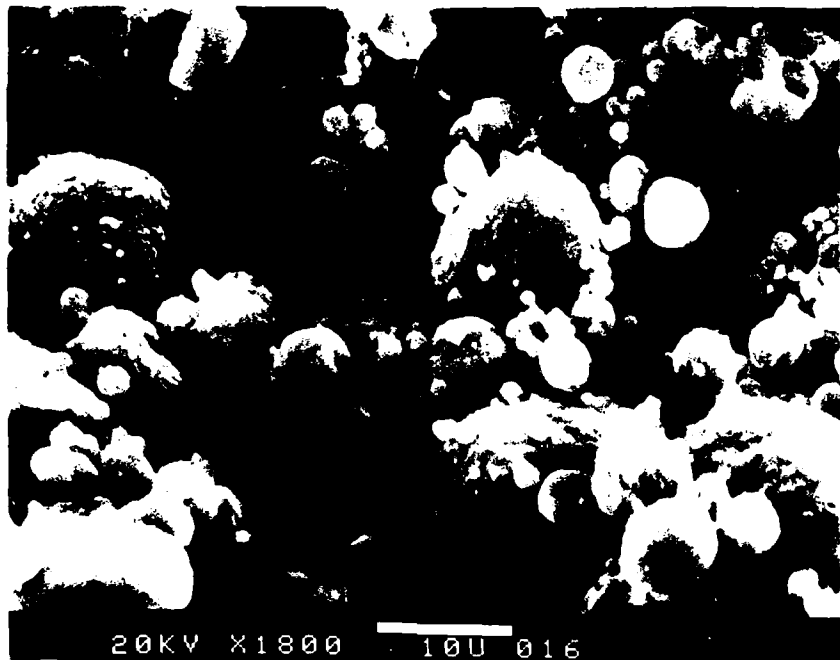
FIGURE 1 - SEM photograph of Atomized Al - 2%Mg.

19
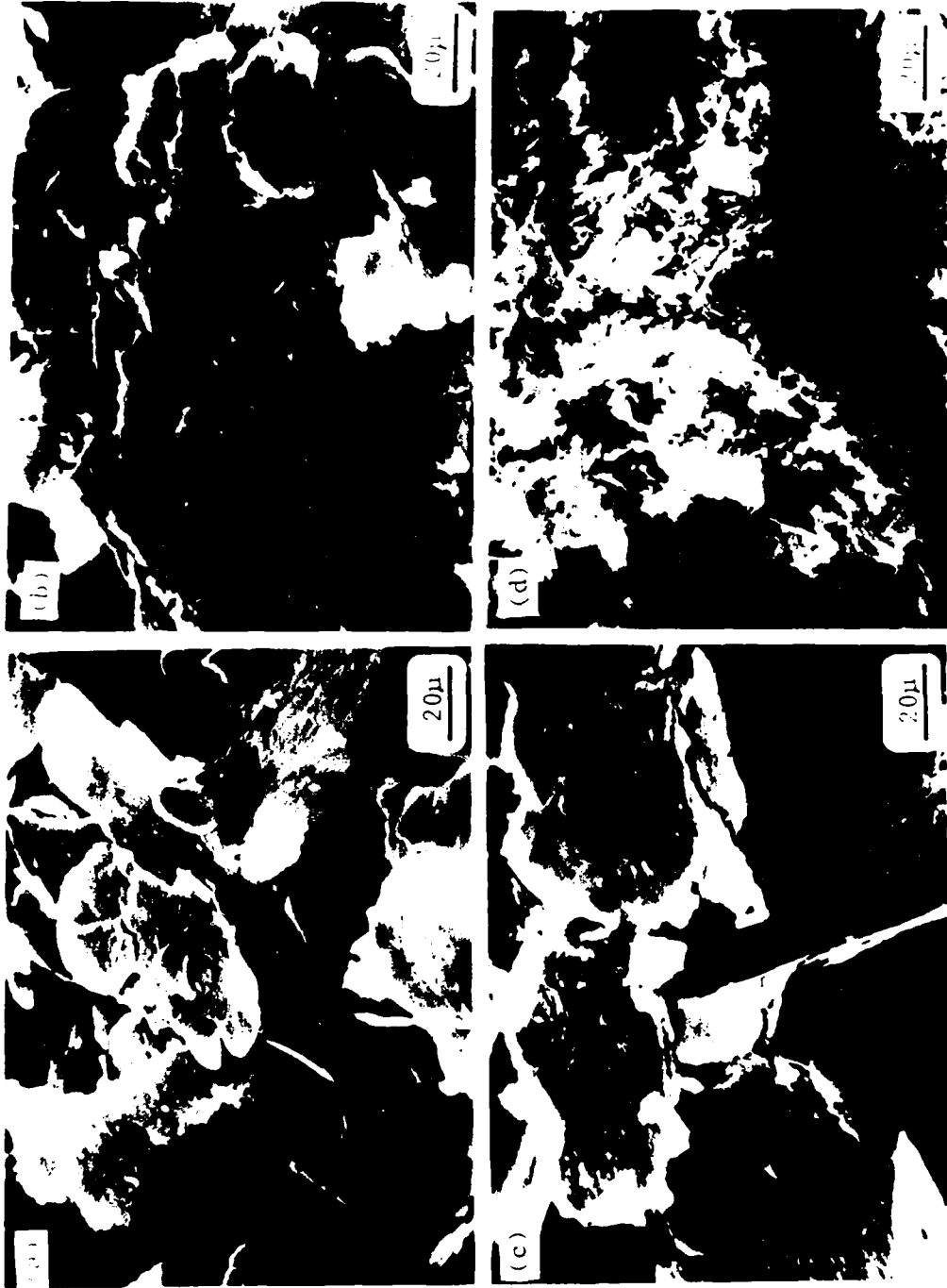
FIGURE 2 - SEM photograph of Attrited Al - 2%Mg Powder.
a.) 1 Hour   b.) 3 Hours   c.) 6 Hours   d.) 12 Hours

20
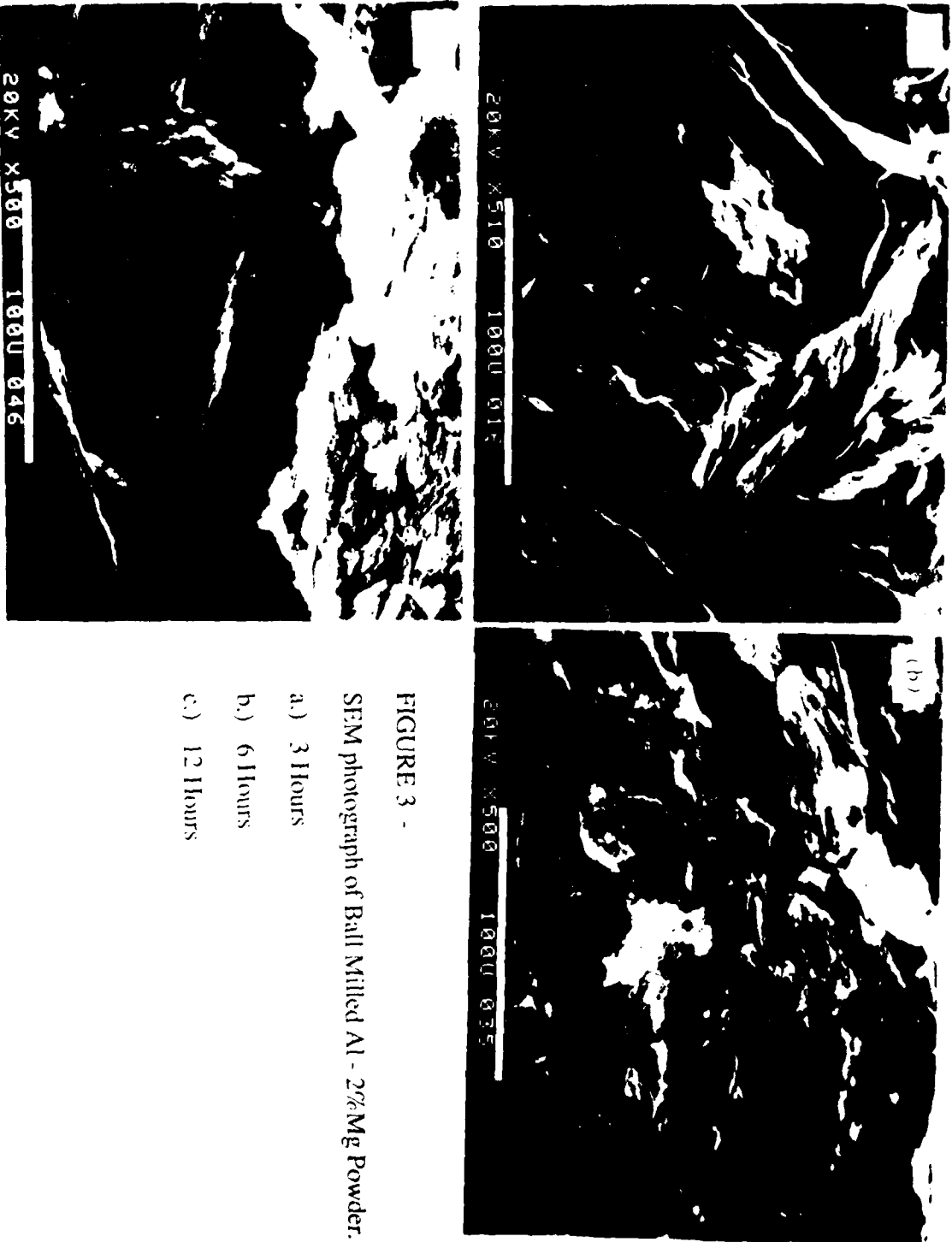
FIGURE 3 -

SEM photograph of Ball Milled Al - 2%Mg Powder.

a.) 3 Hours

b.) 6 Hours

c.) 12 Hours

21
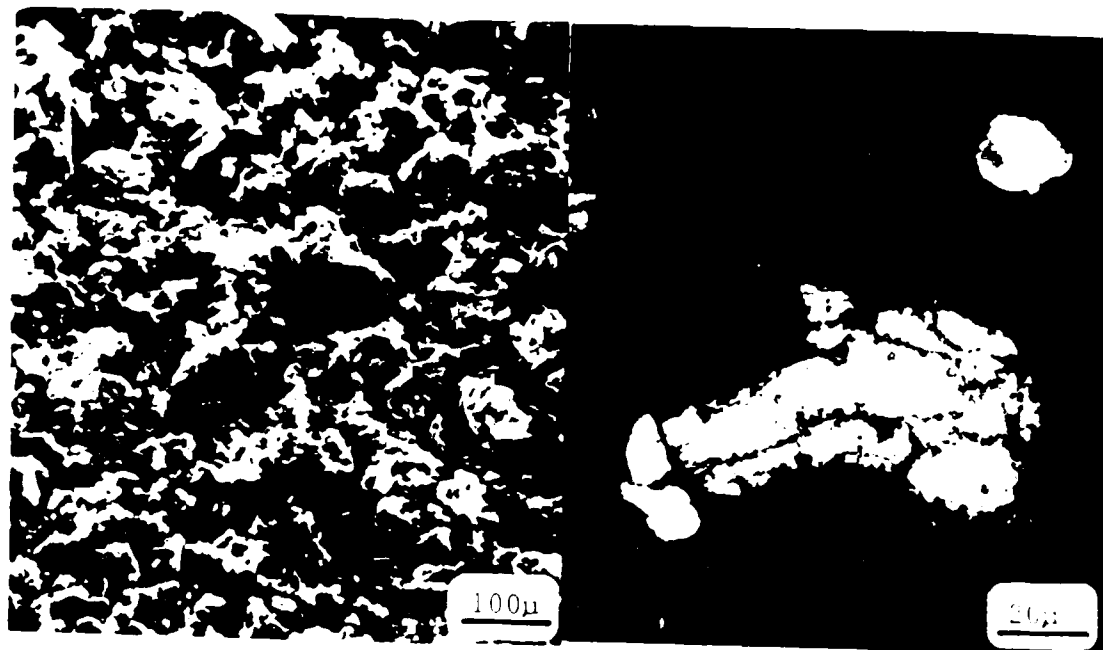
(a) 1 hour
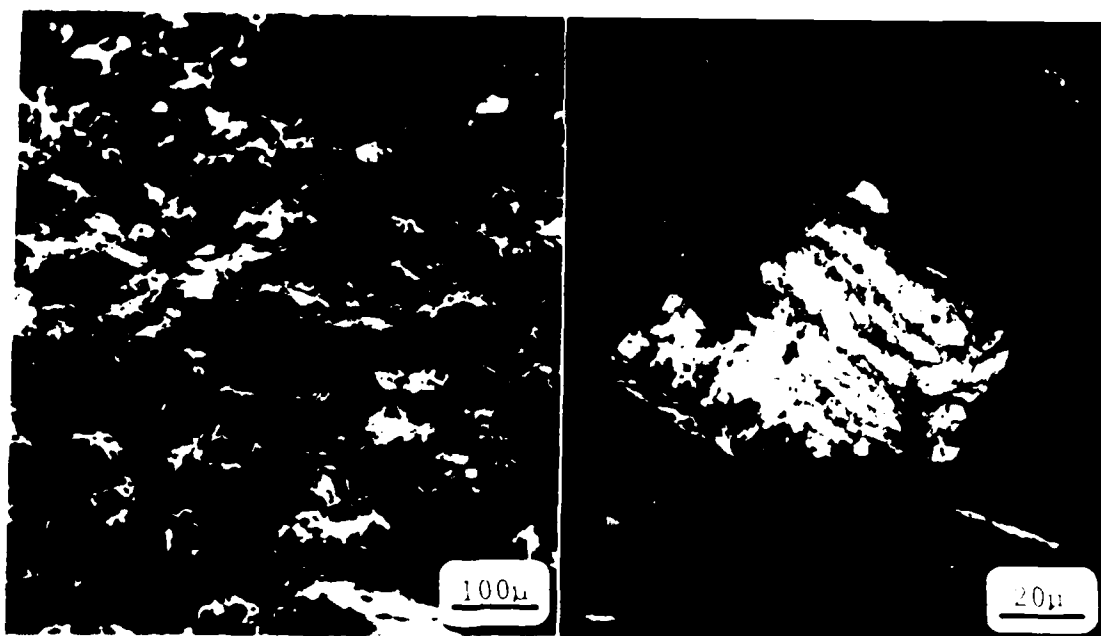
(b) 4 hours

FIGURE 4 - Morphology of 2μm SiC - Al - 2% Mg Powder after Ball Milling for Various Times.
Process control Agent Nopcowax 22 DS

22
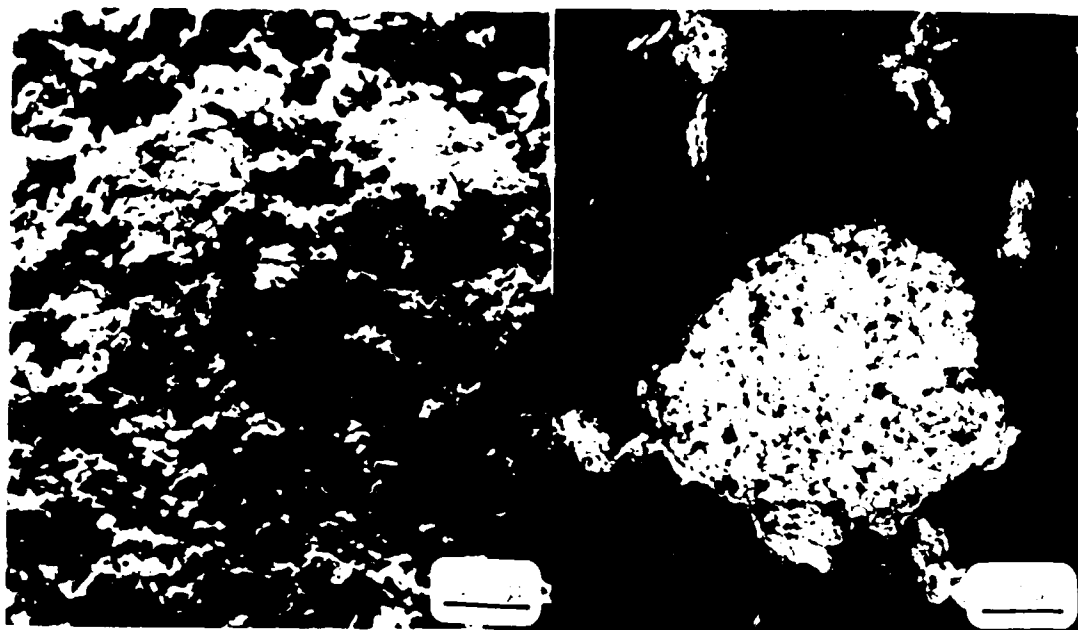
(c) 12 hours
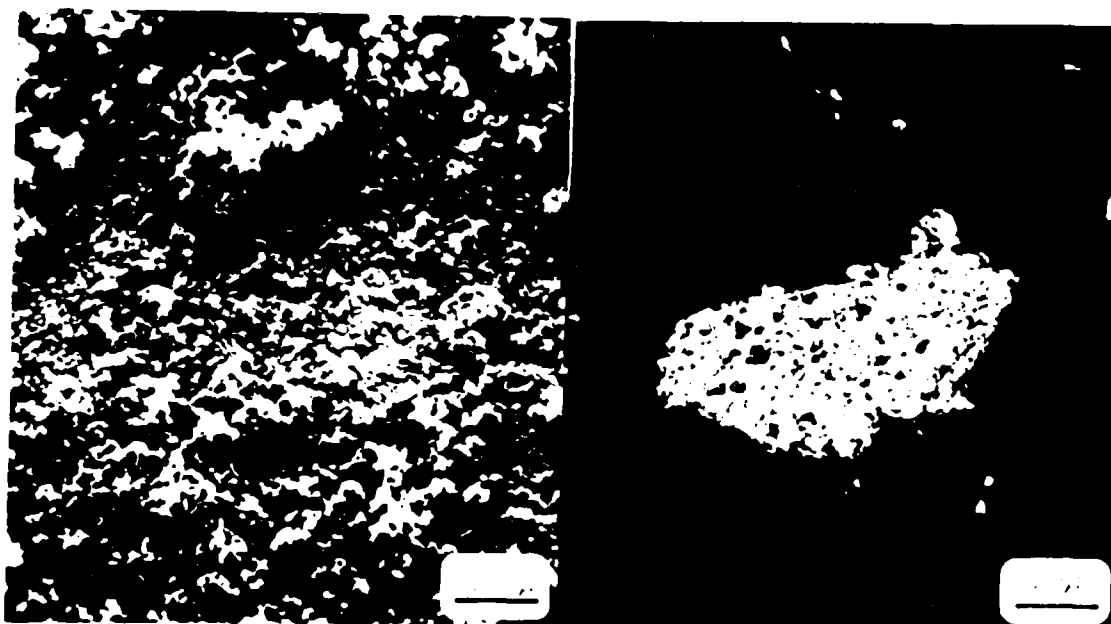
(d) 24 hours

FIGURE 4 - Continued

FIGURE 5 - Aluminum Capsules after (left) and before HIP (right).
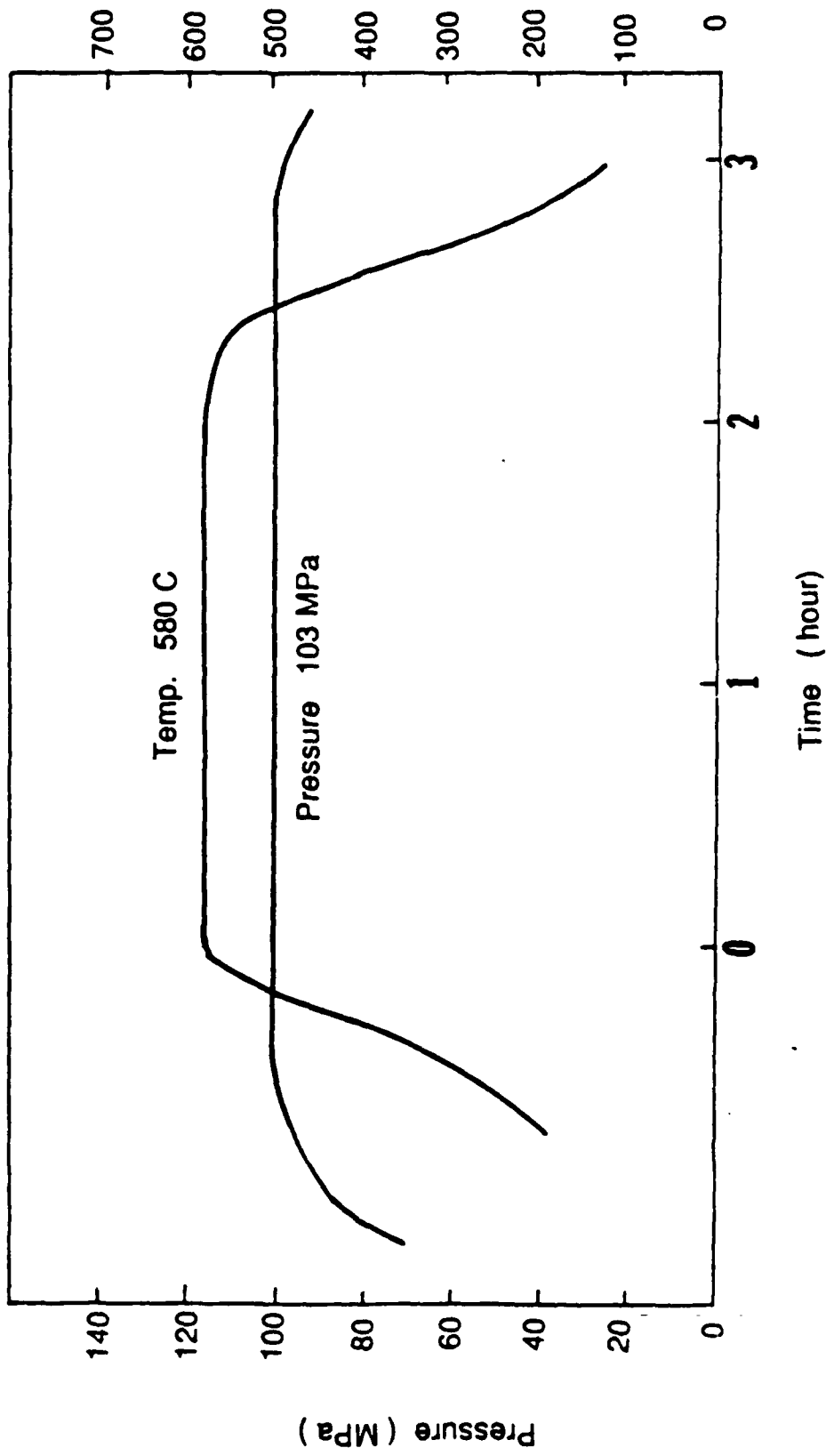
FIGURE 6 - HIP Temperature and Pressure History.

25
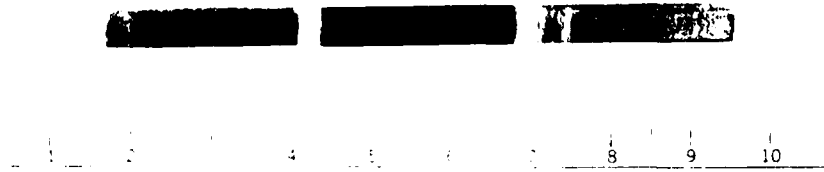
(a) Rectangular type (C-1, C-3~7)

(b) Round type (C-2)

FIGURE 7 - Tensile Test Specimens.
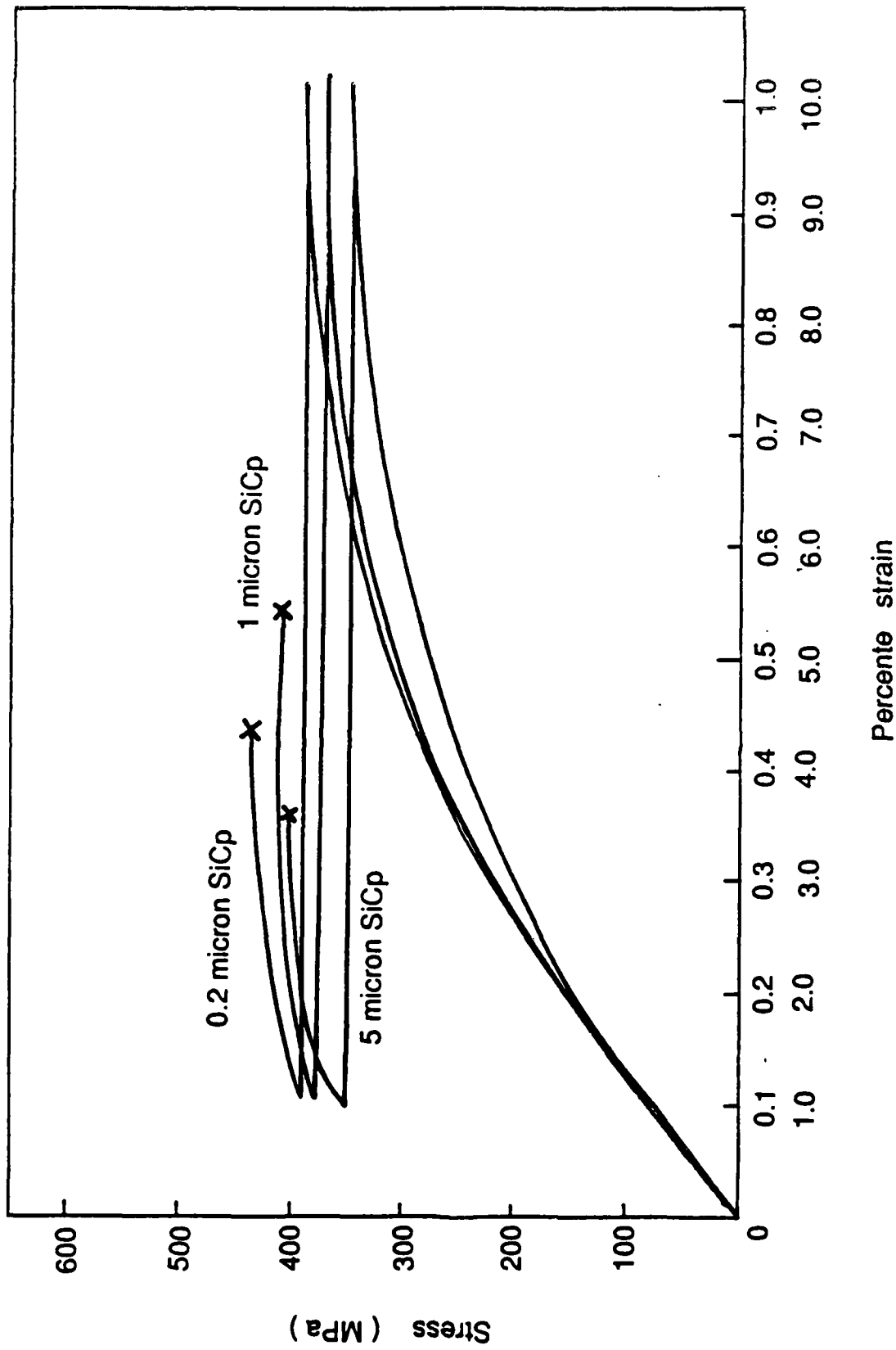
FIGURE 8 - Stress versus strain curves for composites with 10 v/o SiCp reinforcement

27
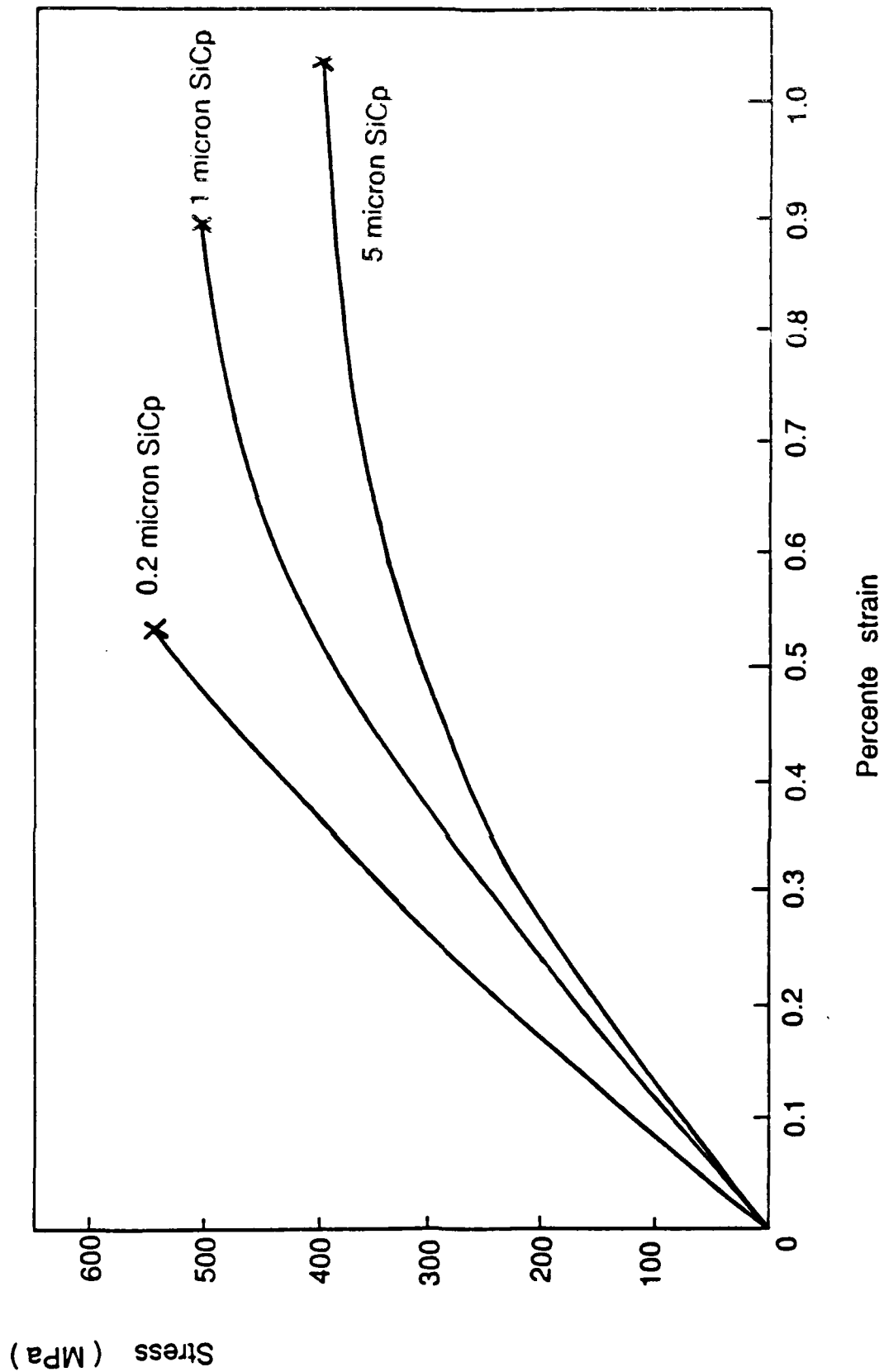
FIGURE 9 - Stress vs. Strain for Composites with 30 % SiC.

28
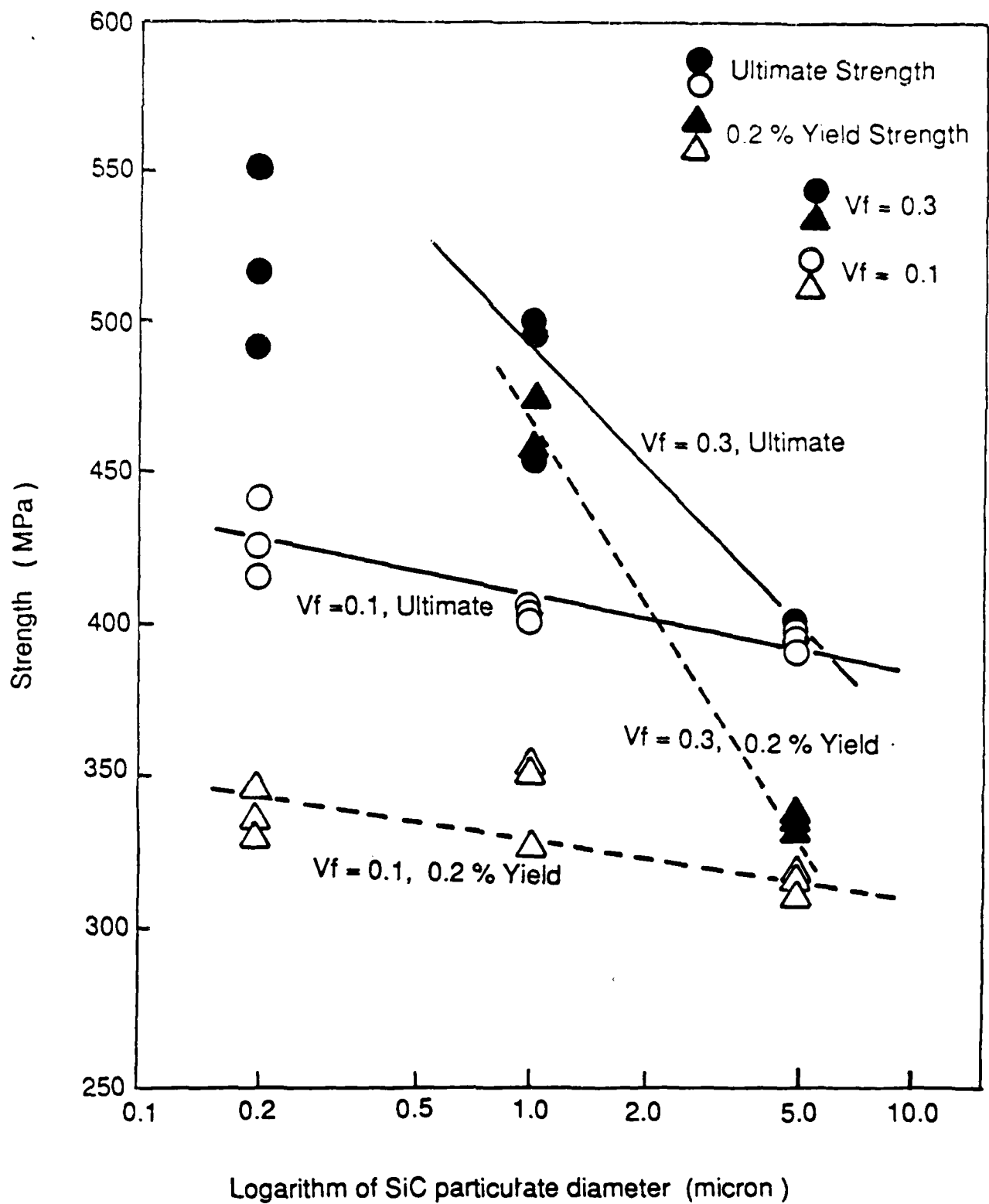
FIGURE 10 - Ultimate End 0.2% Yield Strength vs. Logarithm of SiC Particulate Size.
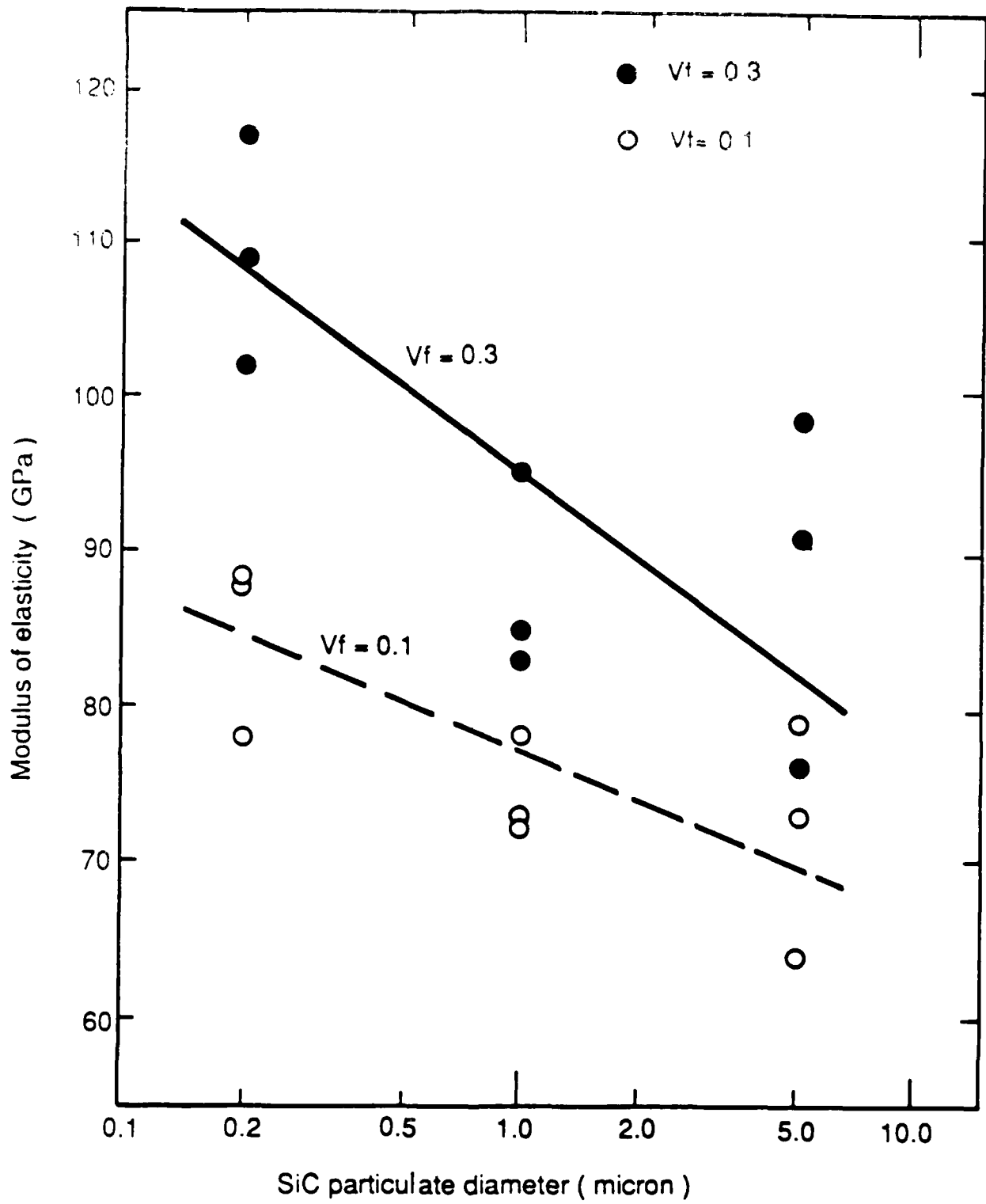
FIGURE 11 - Modulus of Elasticity vs. Logarithm of SiC Particulate Size.
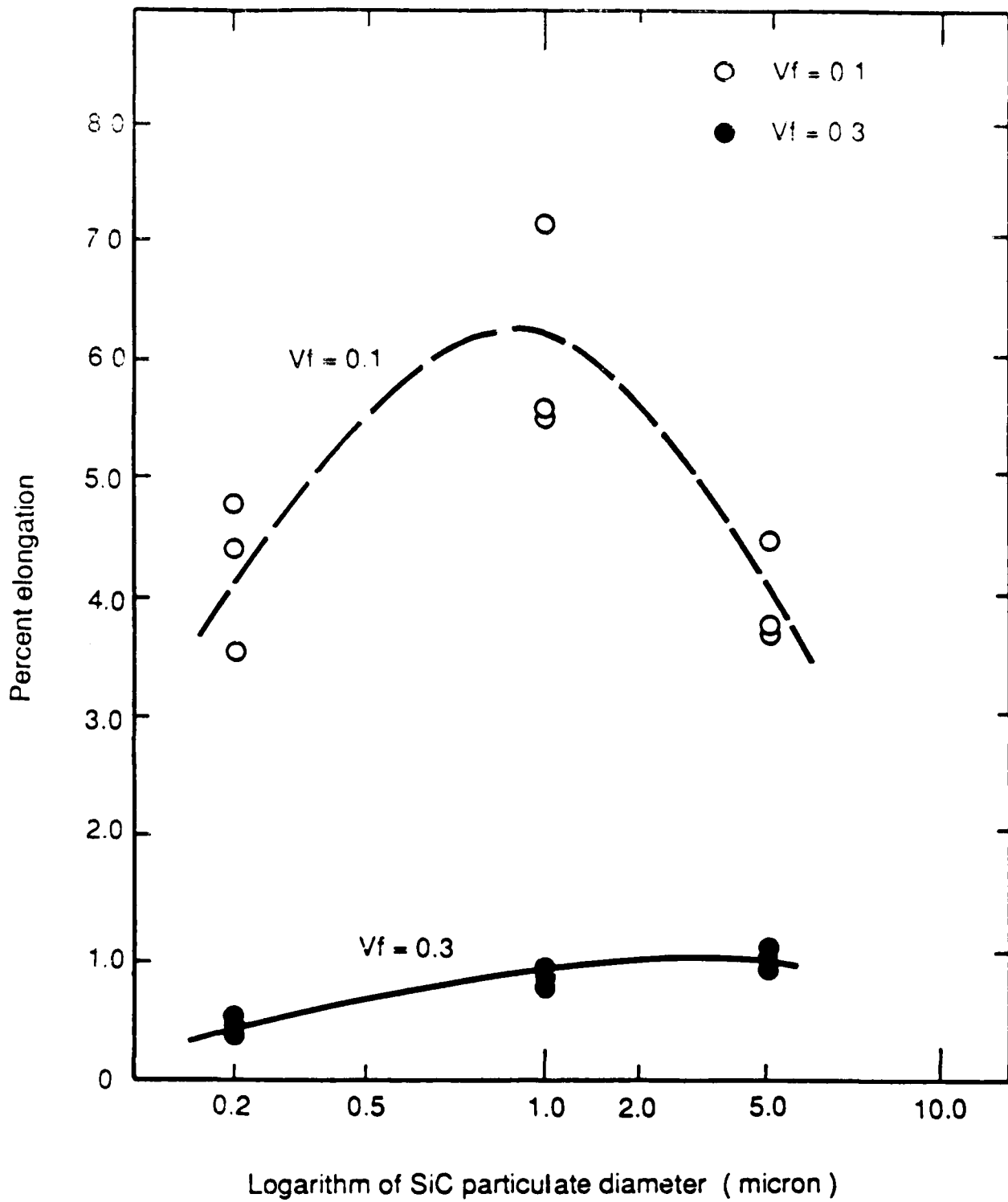
FIGURE 12 - Elongation vs. Logarithm of SiC Particulate Size.
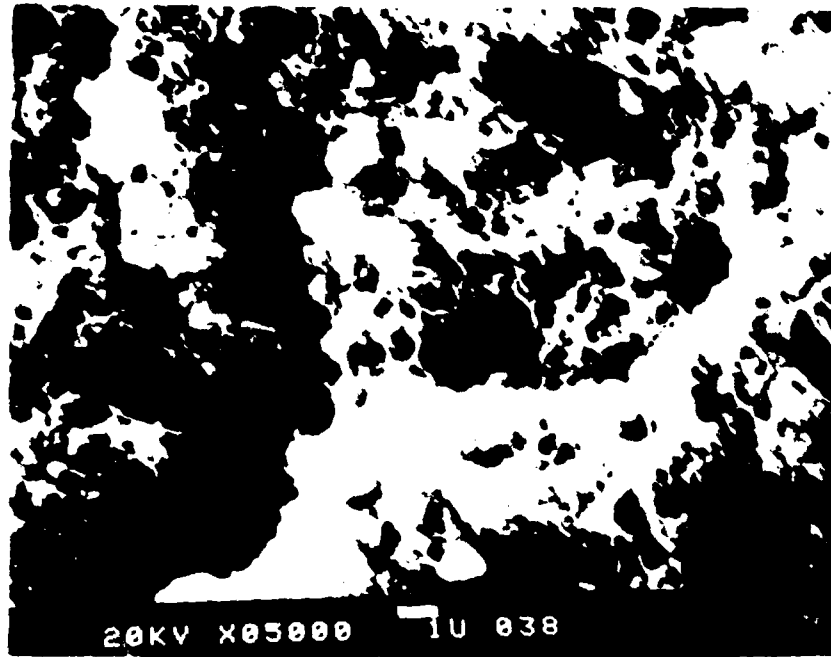
(a) C-5 (0.8 % elongation)

(b) C-1 (3.6 % elongation)

FIGURE 13 - SEM Fractographs Showing Dimples on Extruded Specimens.

32
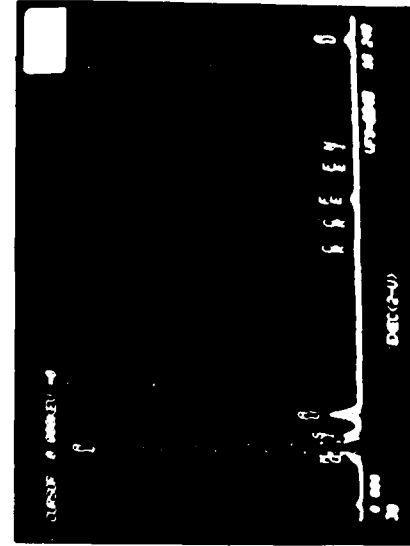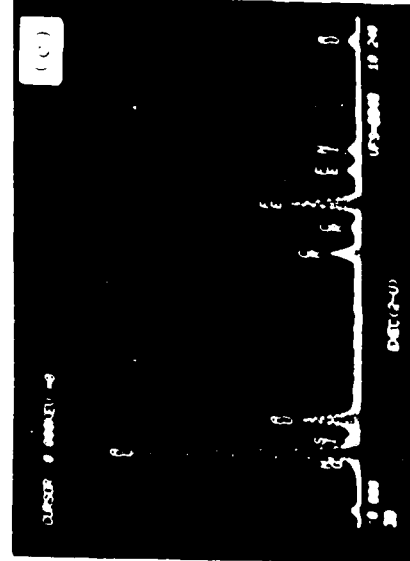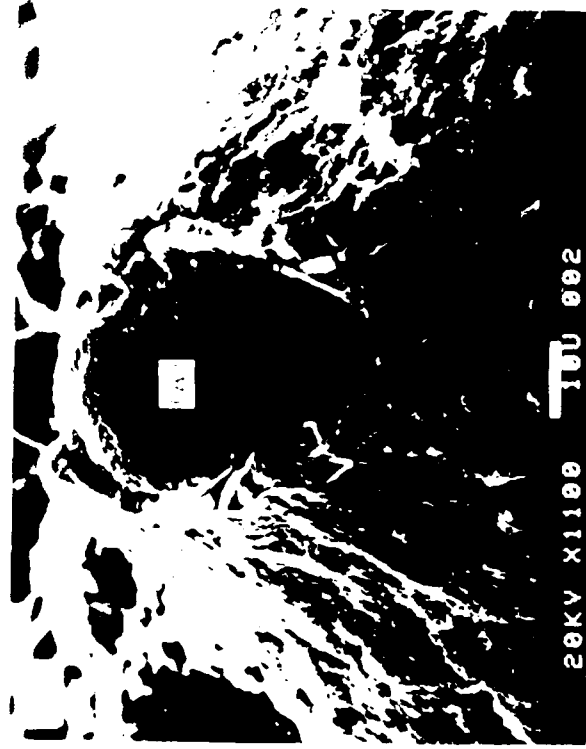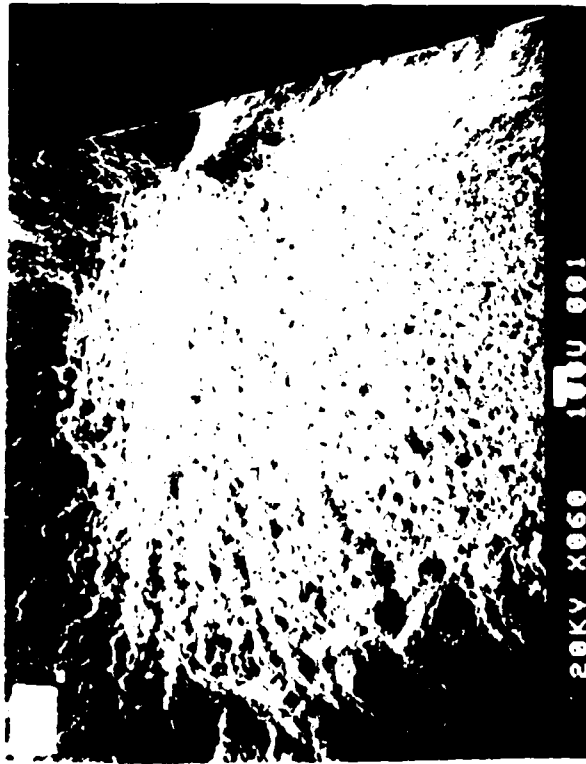
FIGURE 14 - Inclusion as Origin of Failure.

    (a) Low magnification

    (b) High Magnification

    (c) EDAX on (A) in (b)
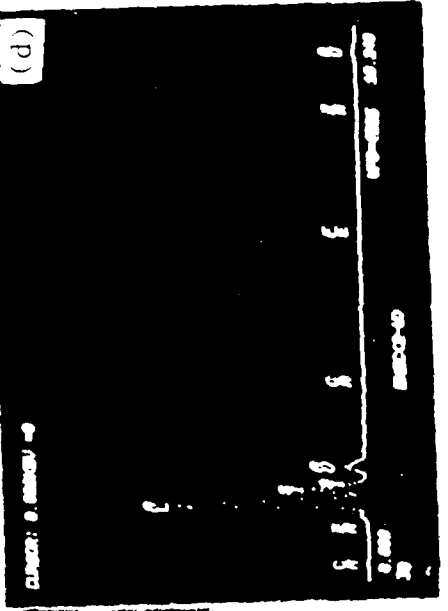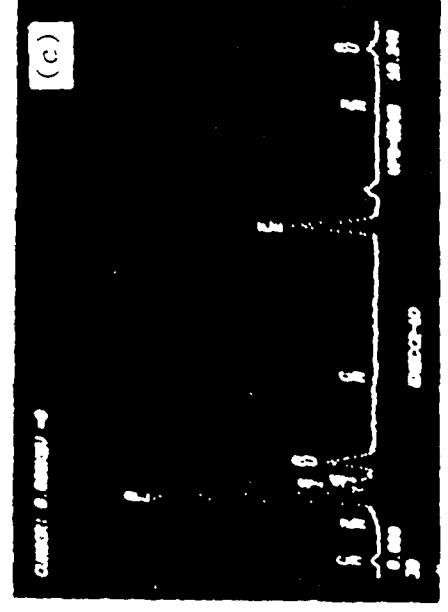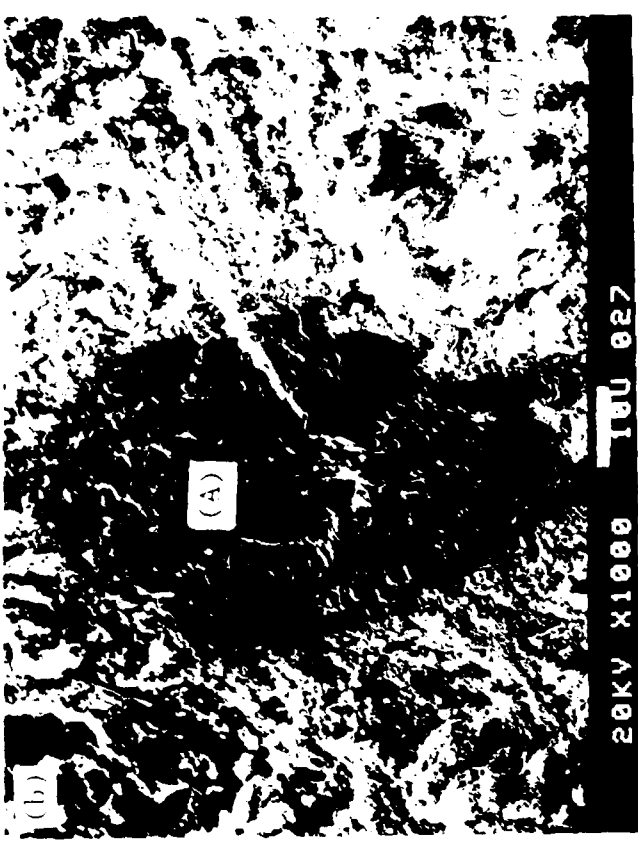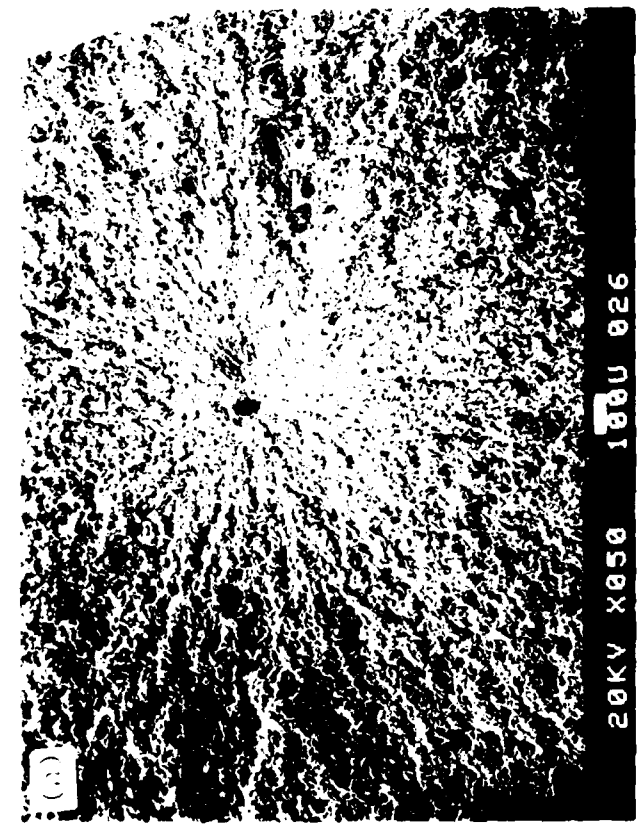
    (d) EDAX on (B) in (b)

FIGURE 15 - Inclusion as Origin of Failure.

(a) Low magnification

(b) High Magnification

(c) EDAX on (A) in (b)

(d) EDAX on (B) in (b)

34

20KV X18   1000U 147

20KV X3000   10U 146
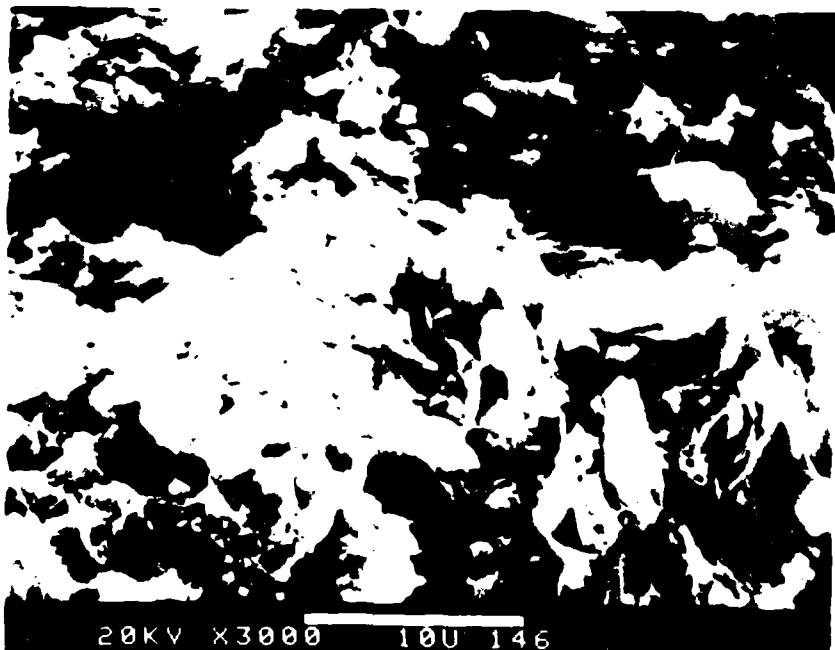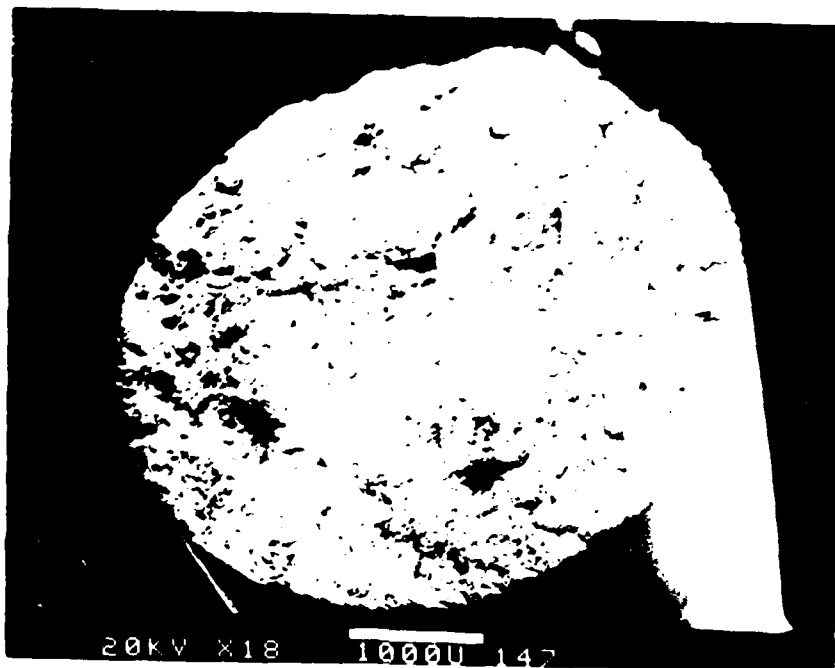
FIGURE 16 - SEM fractographs of as HIPed C-2
composite
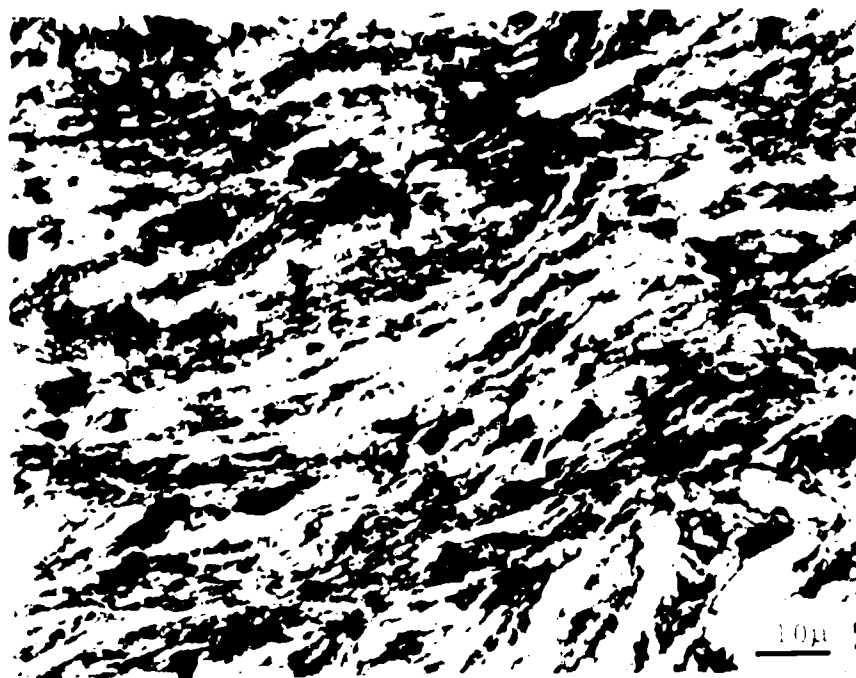
(a) 10 v o 5 micron SiCp

FIGURE 17 - Microstructures of as HIP-ed Composites.
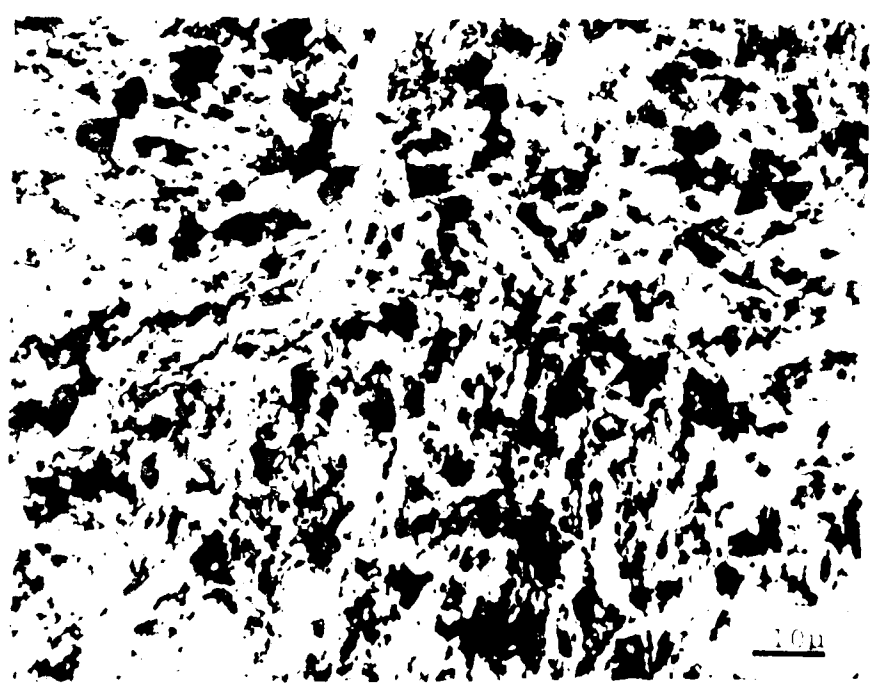
(b) 20 v/o 5 micron SiCp

FIGURE 17 - Continued
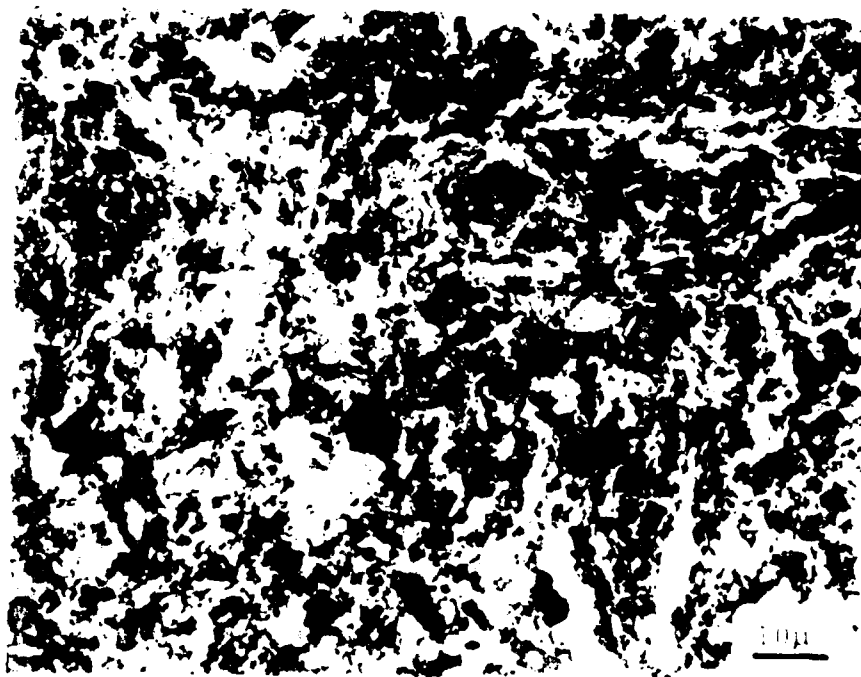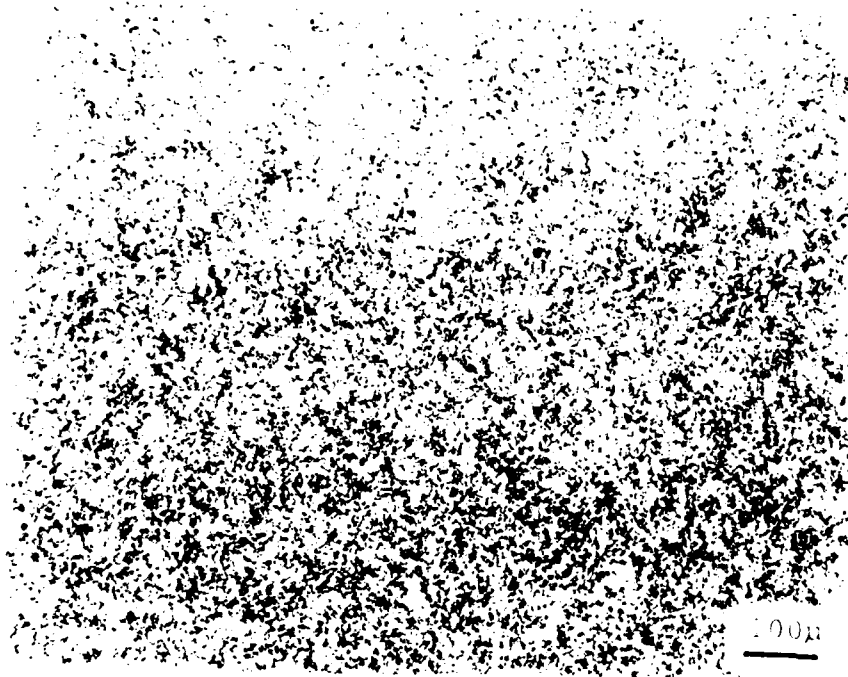
(c) 30 v/o 5 micron SiCp

FIGURE 17 - Continued
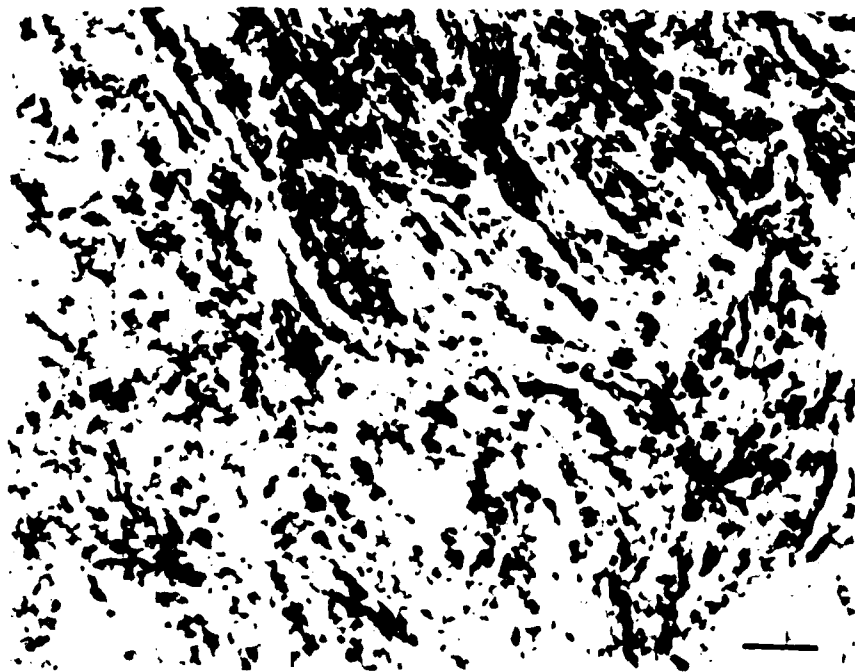
c 10 vo 1 micron S Cp

FIGURE 17 - Continued

（）30 v o 1 micron SiCp

FIGURE 17 - Continued

40

(f) 10 v/o 0.2 micron SiCp

FIGURE 17 - Continued

41
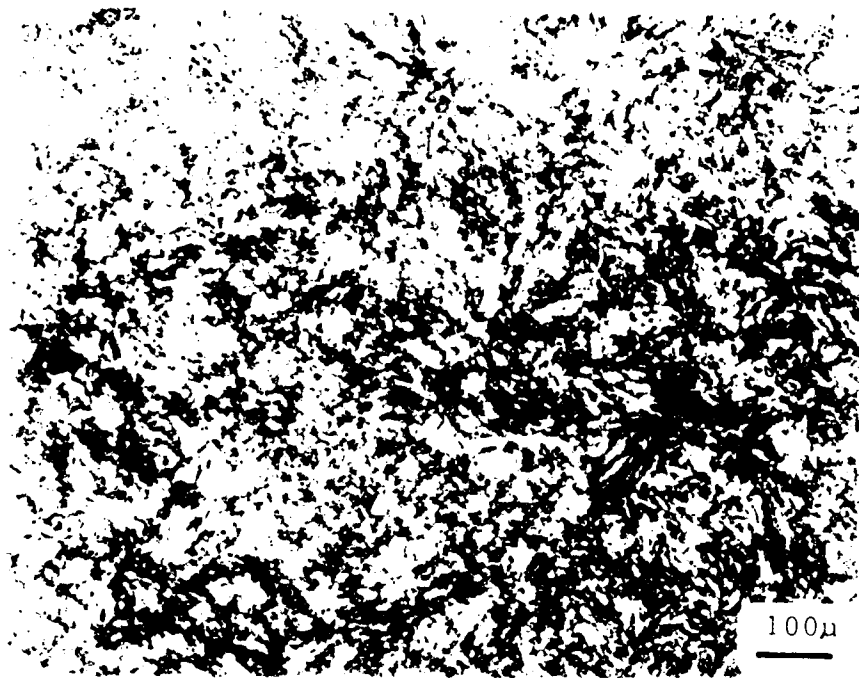
(g) 30 v/o 0.2 micron SiCp

FIGURE 17 - Continued

(a) 10 v'o 5 micron SiCp

FIGURE 18 - Microstructures of Extruded Composites.

43

(c) 30 v/o 5 micron SiCp

FIGURE 18 - Continued

45
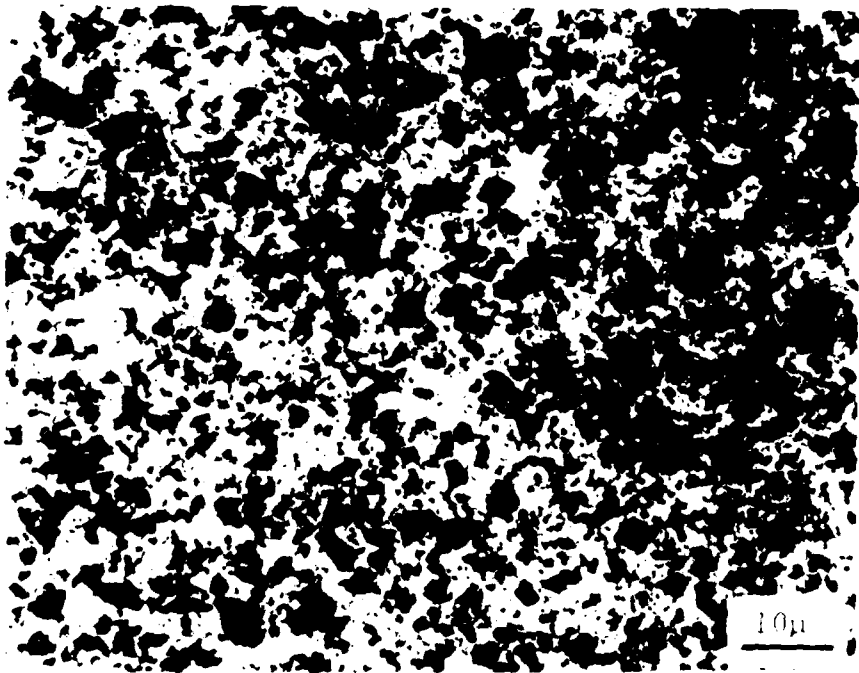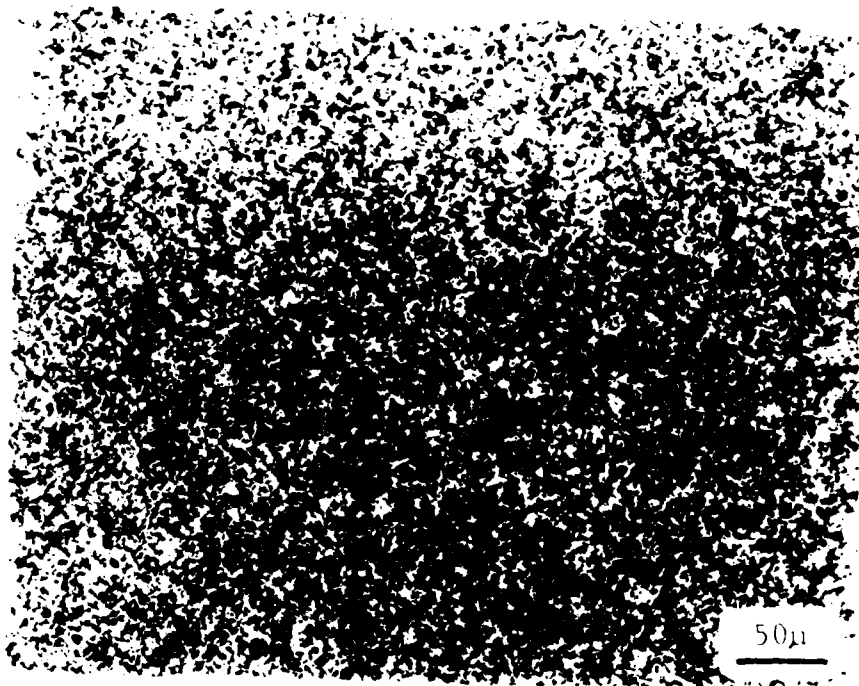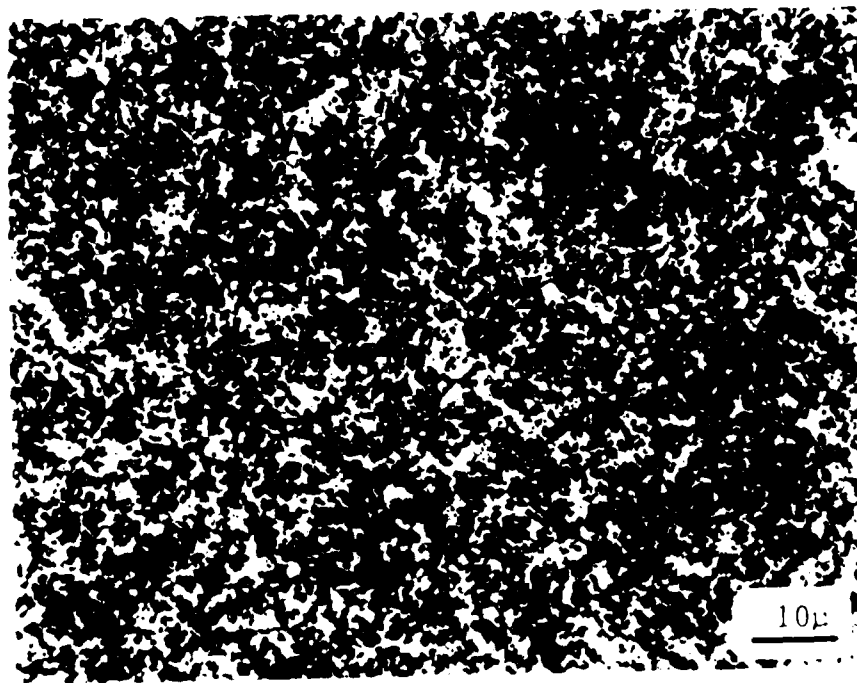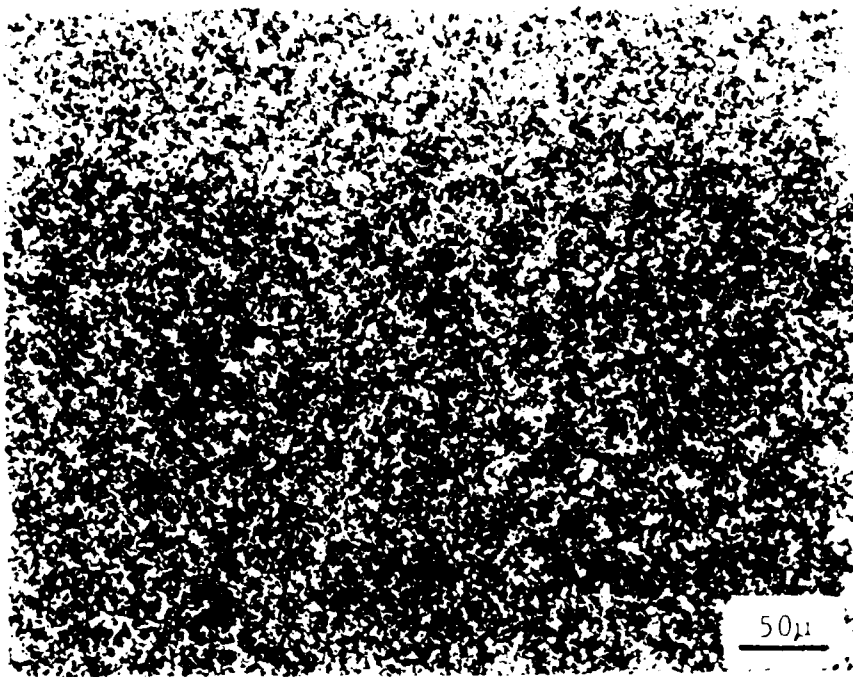
(d) 10 v/o 1 micron SiCp

FIGURE 18 - Continued

46
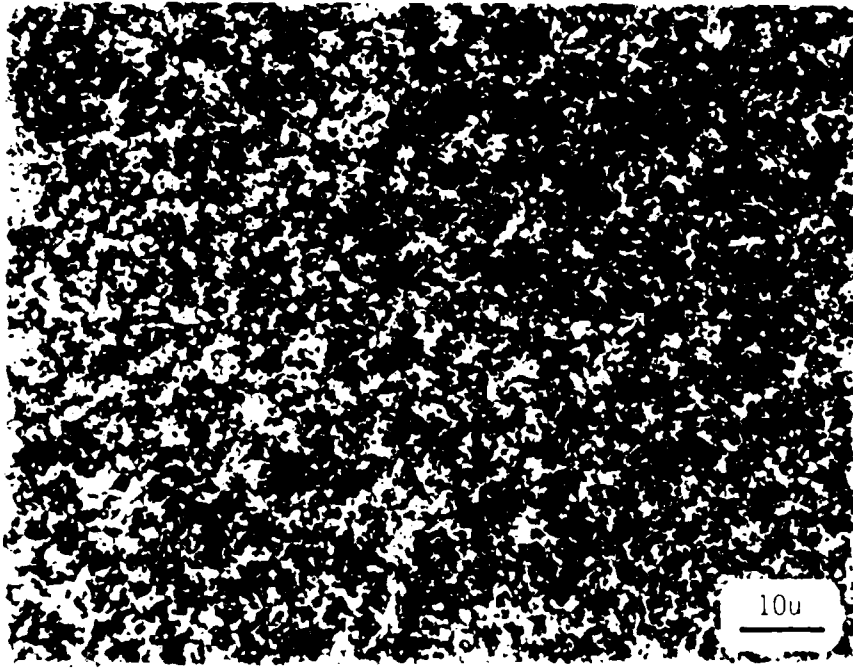
(e) 30 v/o 1 micron SiCp

FIGURE 18 - Continued

47
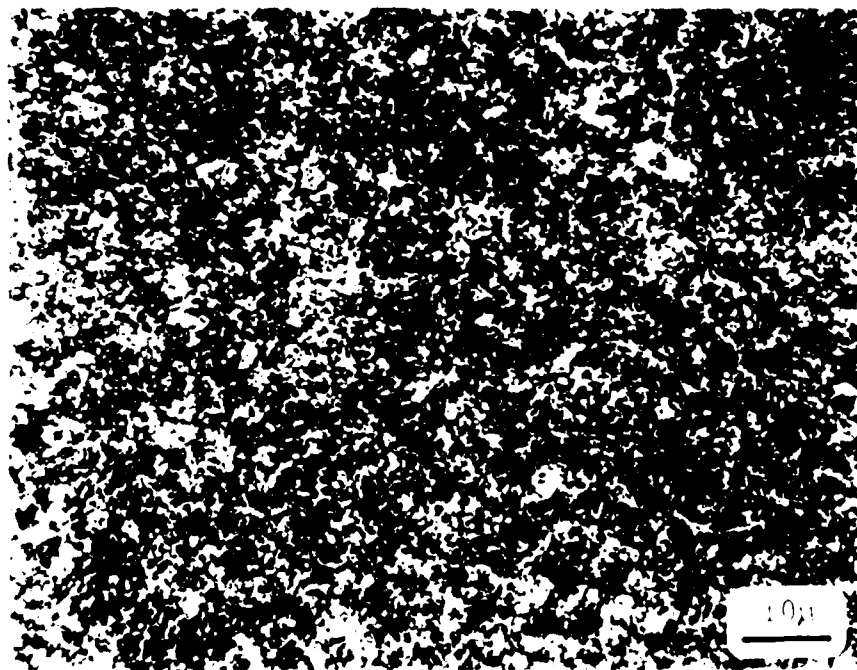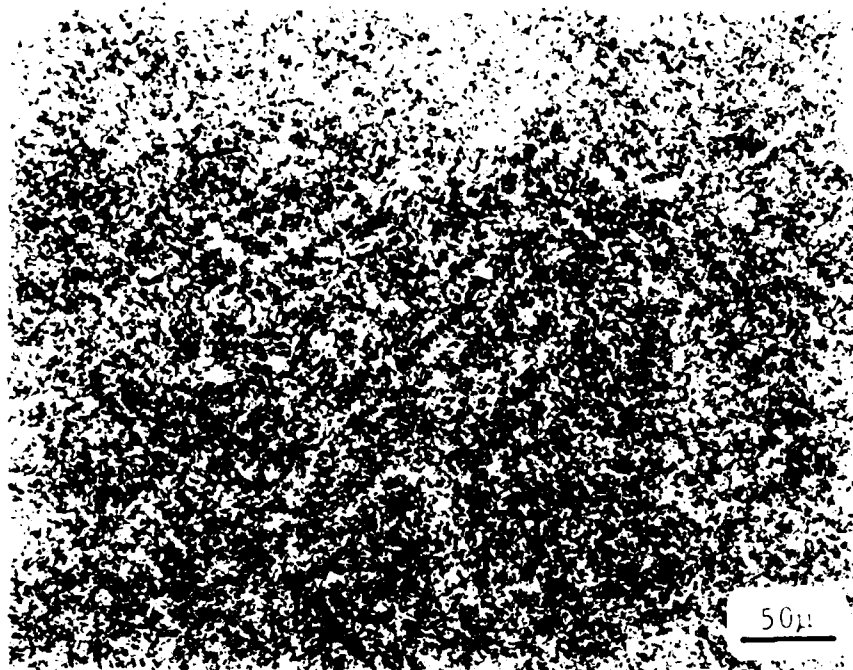
(f) 10 v/o 0.2 micron SiCp

FIGURE 18 - Continued

(g) 30 v/o 0.2 micron SiCp

FIGURE 18 - Continued

49
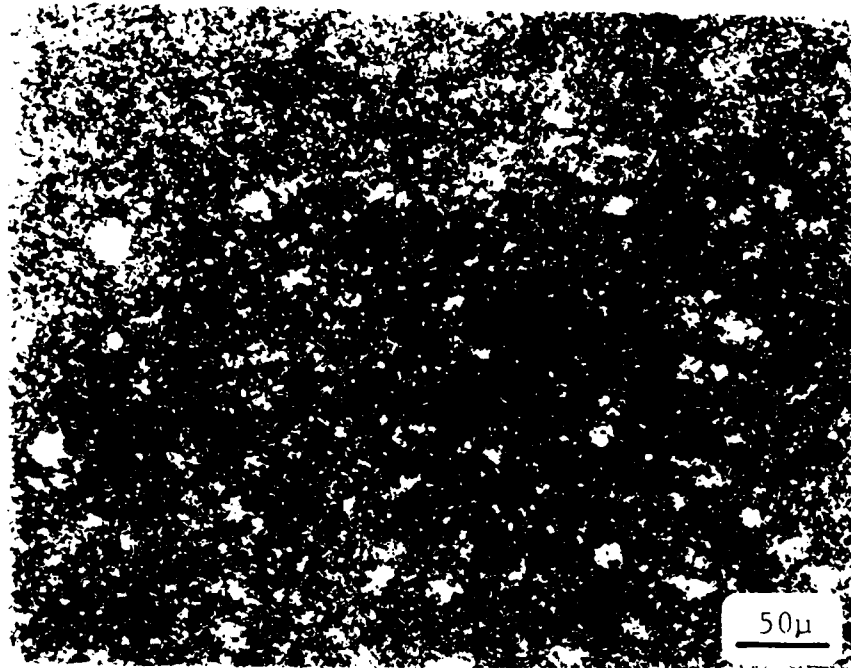
FIGURE 19 - Distribution of 10% 5μm SiC.

FIGURE 20 - Distribution of 20% 5μm SiC.
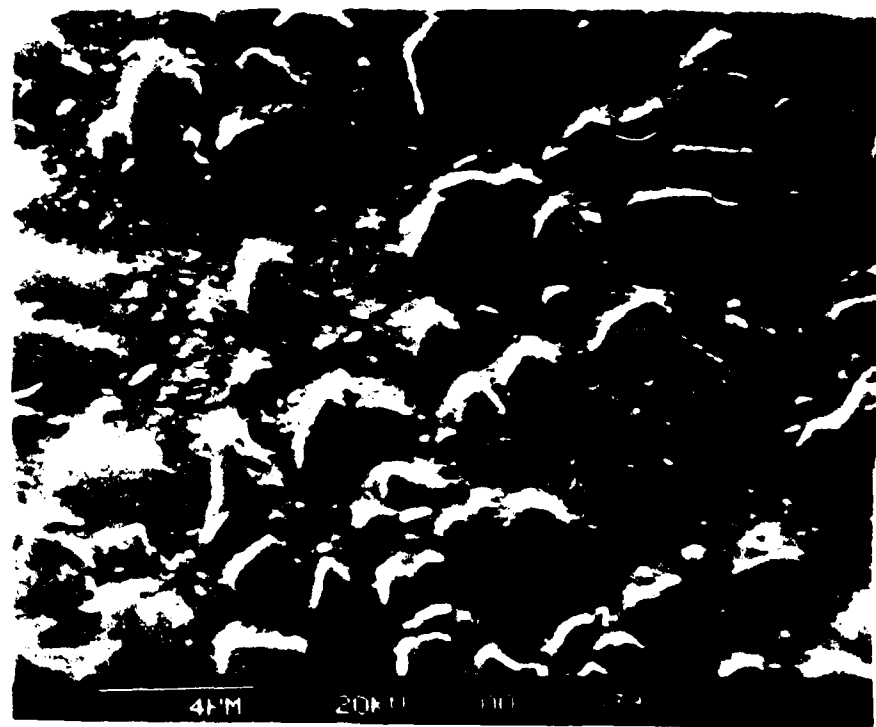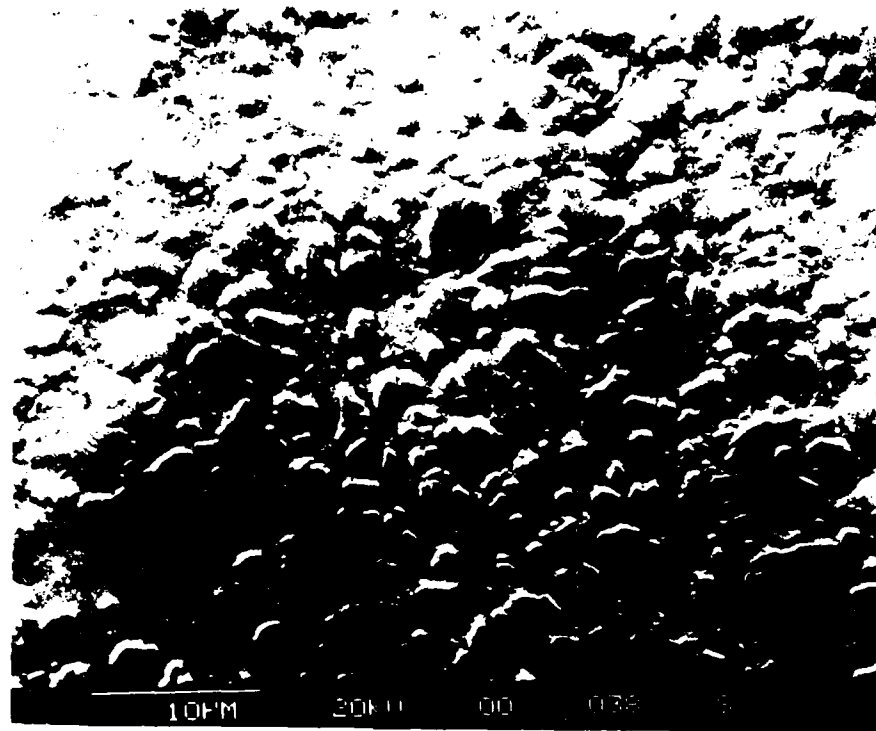
FIGURE 21 - Distribution of 30% 5μm SiC.
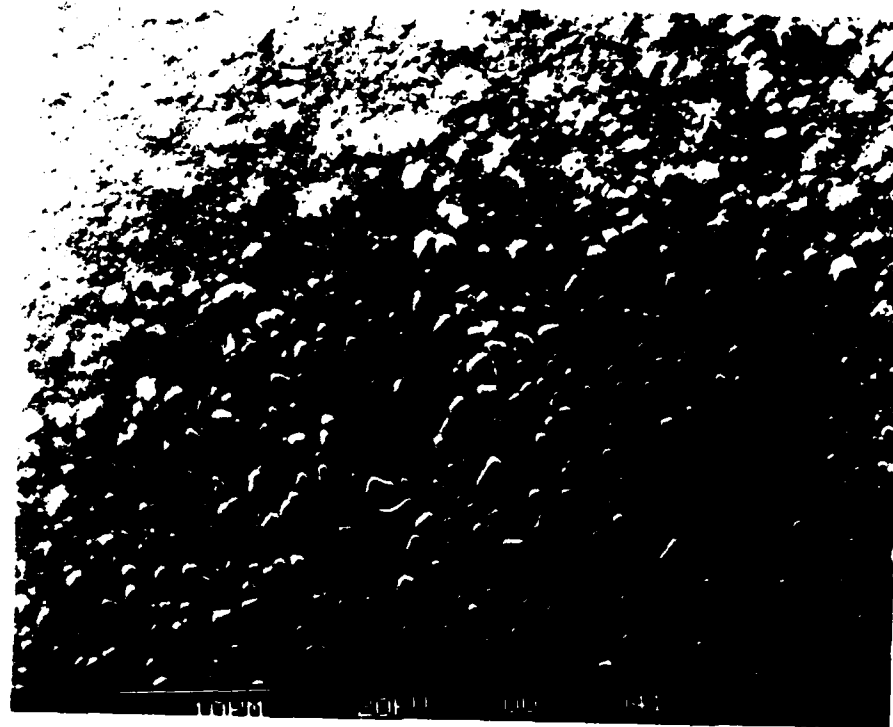
FIGURE 22 - Distribution of 10% 1μm SiC.

54
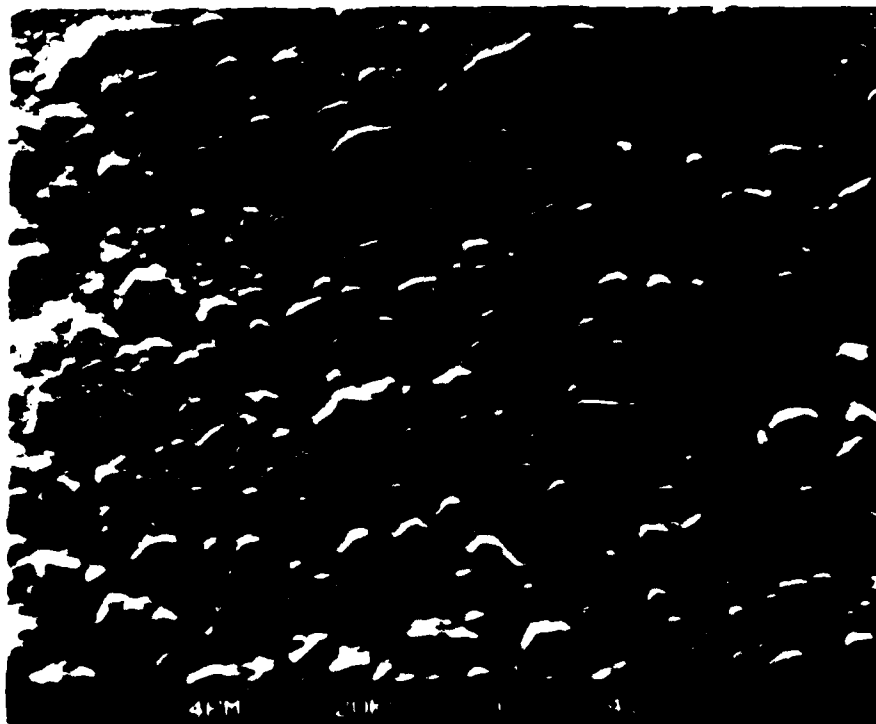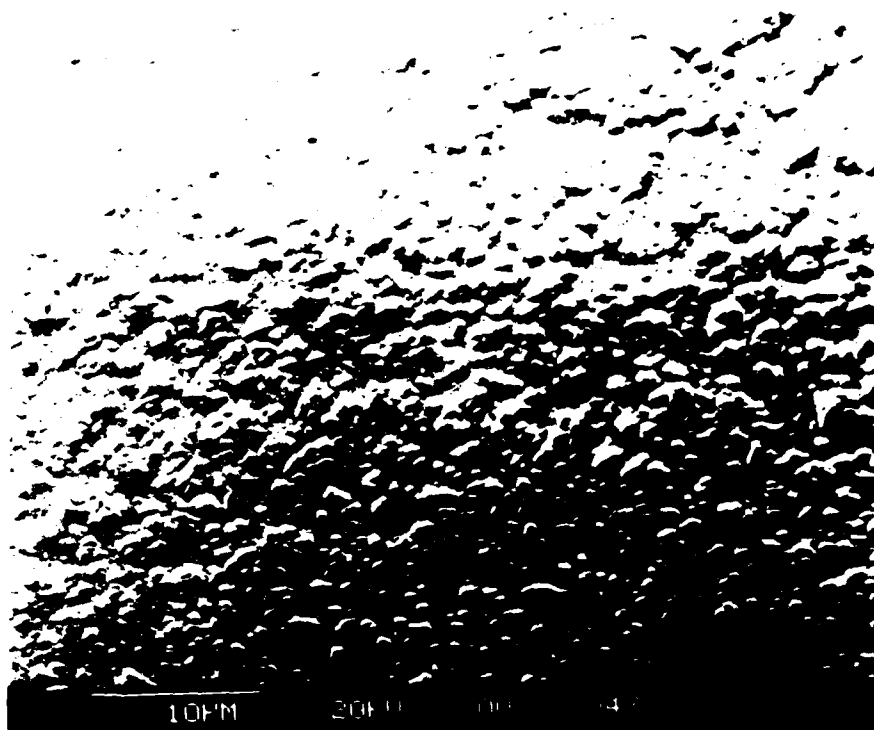
FIGURE 23 - Distribution of 30% 1μm SiC.

FIGURE 24 - TEM Micrograph on the Distribution of 10% 0.2μm SiC in as HIP-ed State.
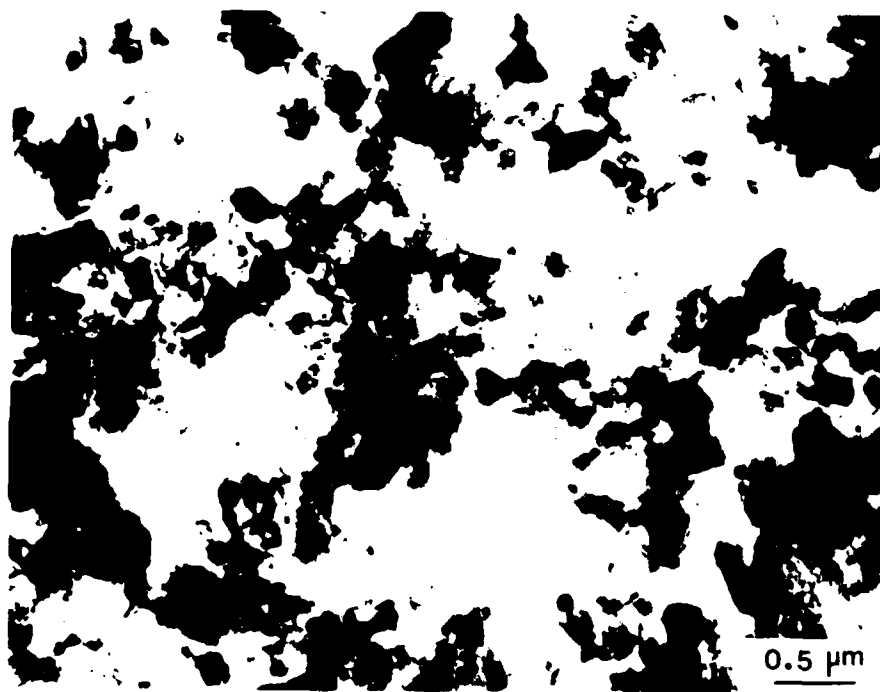
FIGURE 25 - TEM Micrograph on the Distribution of 10% 0.2 μm SiC in as Extruded State.
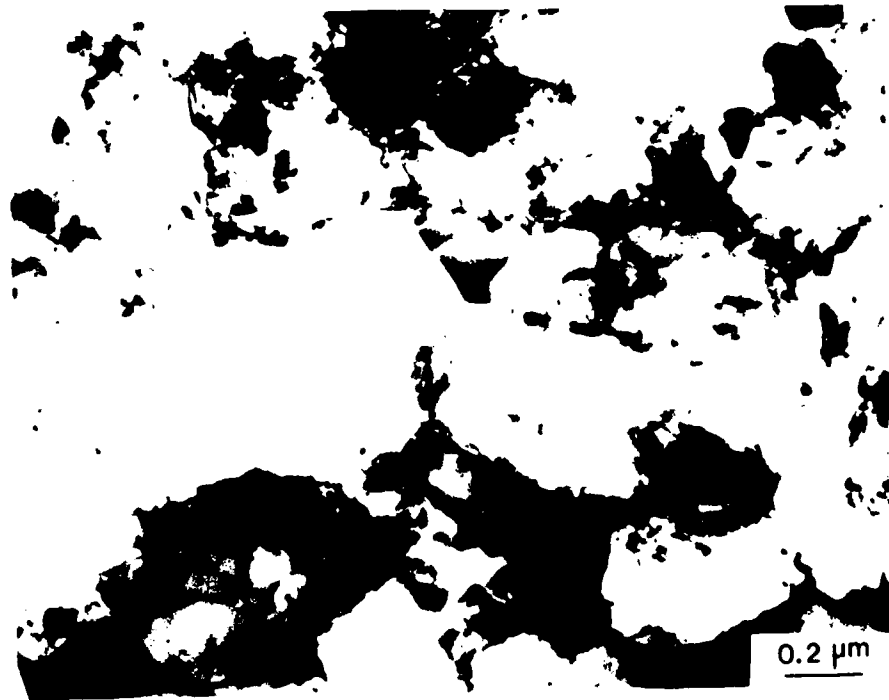
FIGURE 26 - TEM Micrograph on the Distribution of Second Phase Particles.

10 nm

FIGURE 27 - STEM Micrograph of the Mg and Oxygen Rich Second Phase Particles in the 10% 0.2μm SiC Composite.
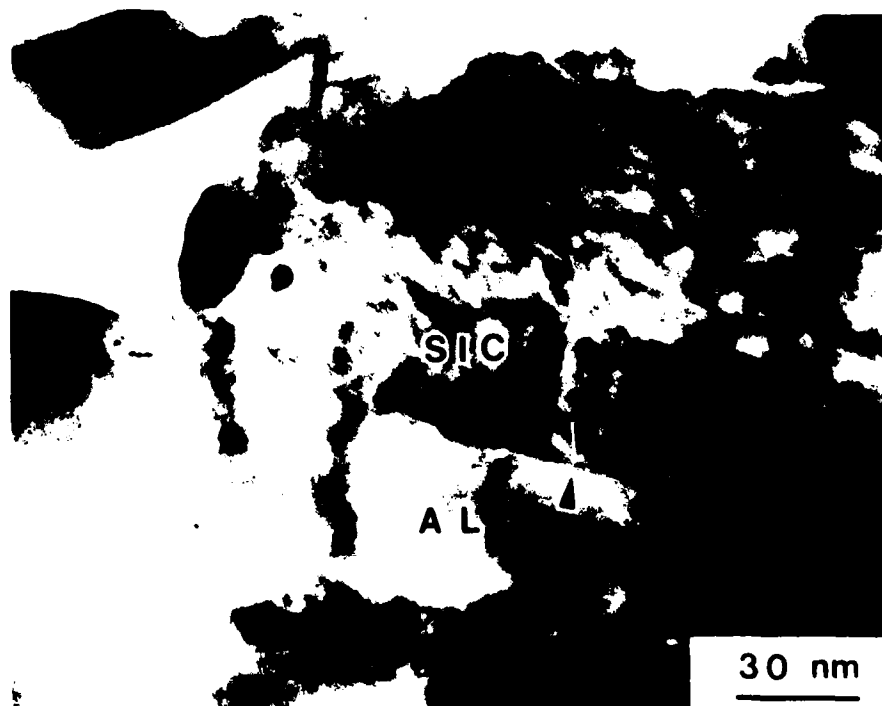
FIGURE 28 - STEM Micrograph Showing SiC/Al Interface in the 10% 0.2μm SiC Composite.
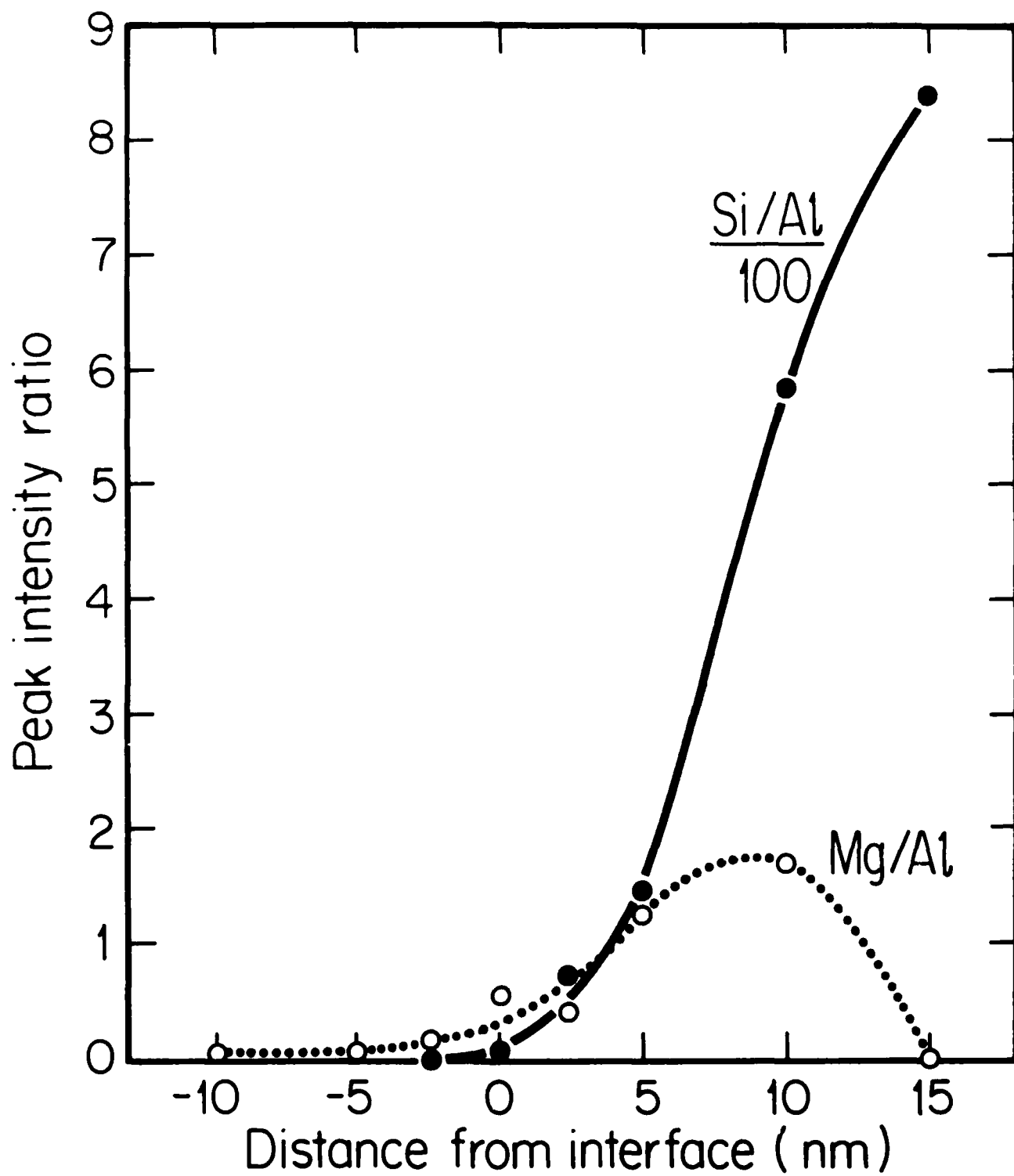
FIGURE 29 - Compositional Variation of the SiC - Al Interface Shown in figure 28.
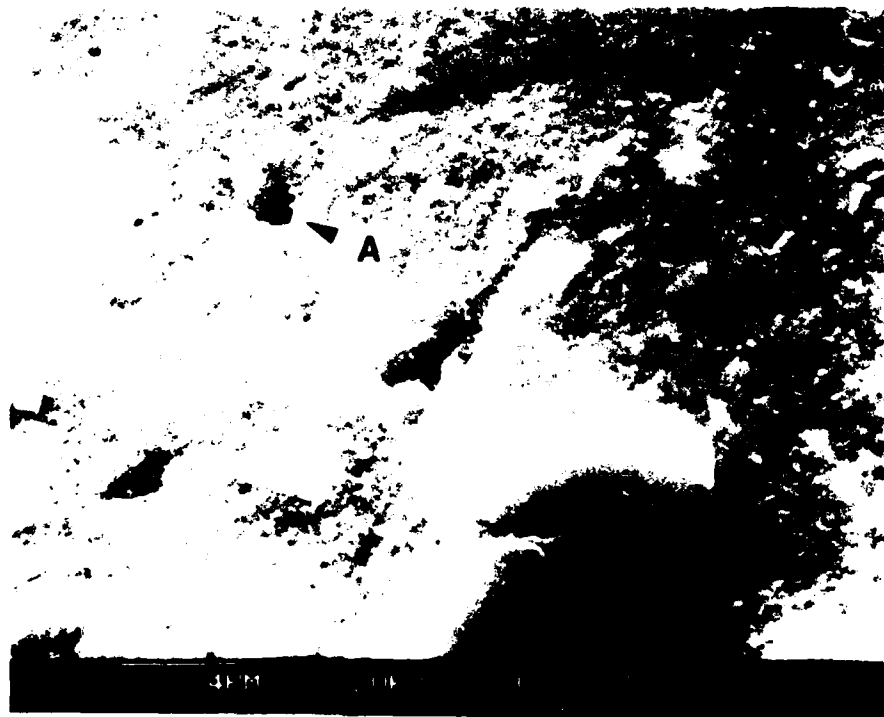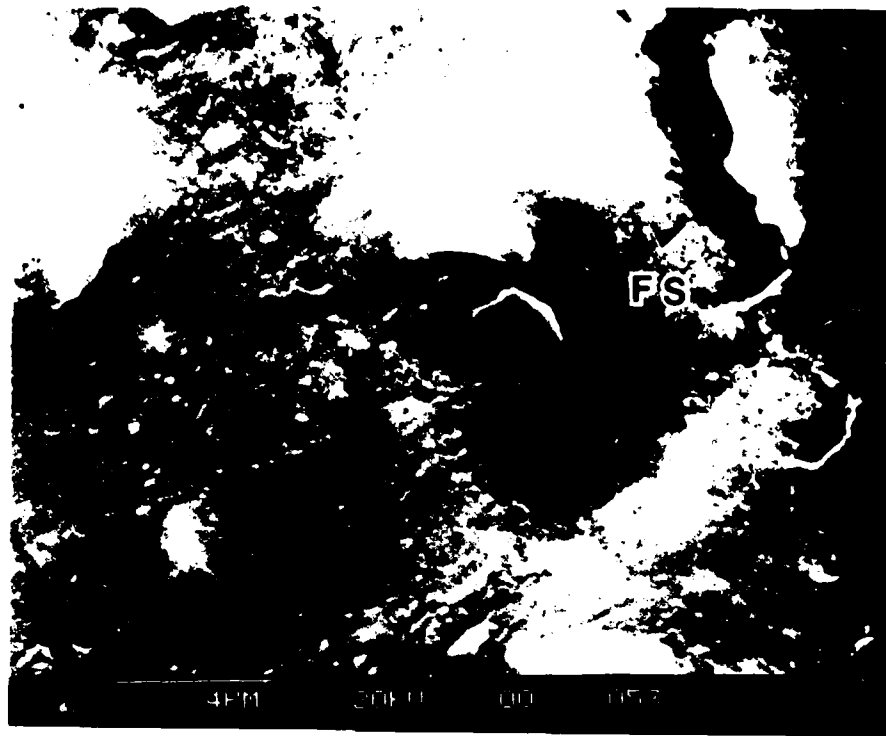
FIGURE 30 - SEM Micrograph of the Region Beneath the Tensile Fracture Surface in the 5-10 Composite.
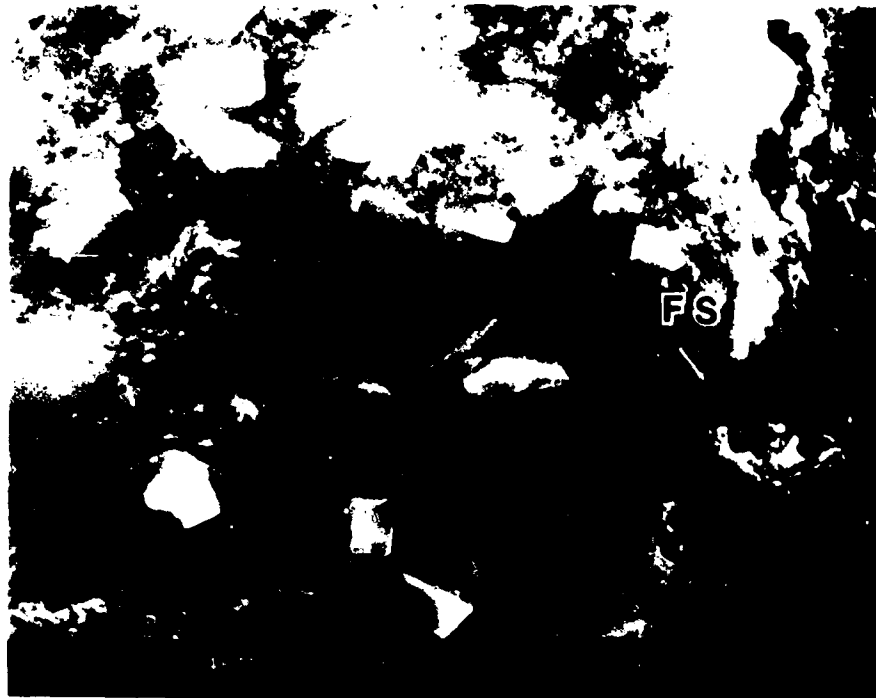
FIGURE 31 - SEM Micrograph of the Region Beneath the Tensile Fracture Surface in the 5-30 Composite.
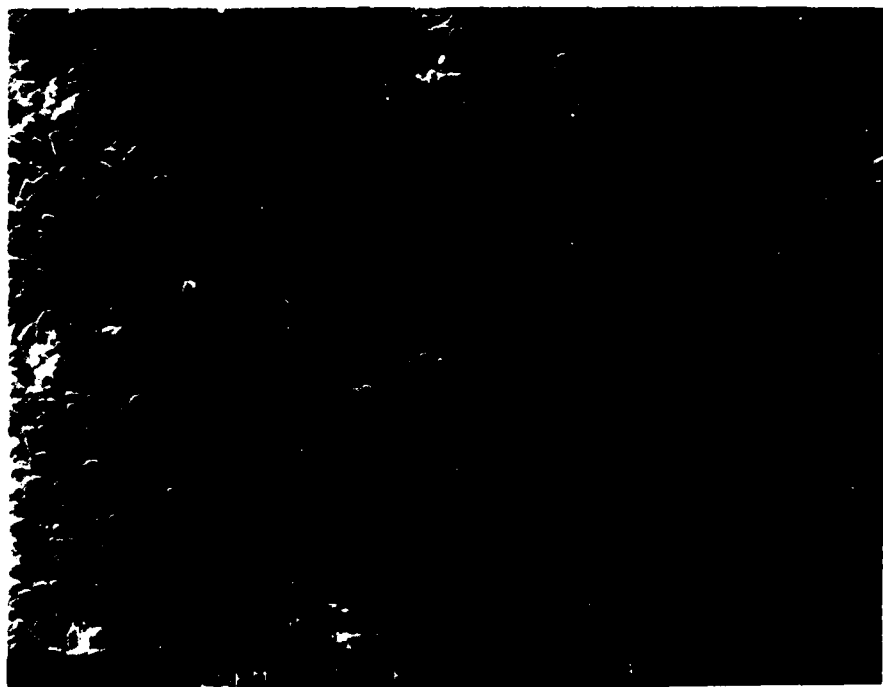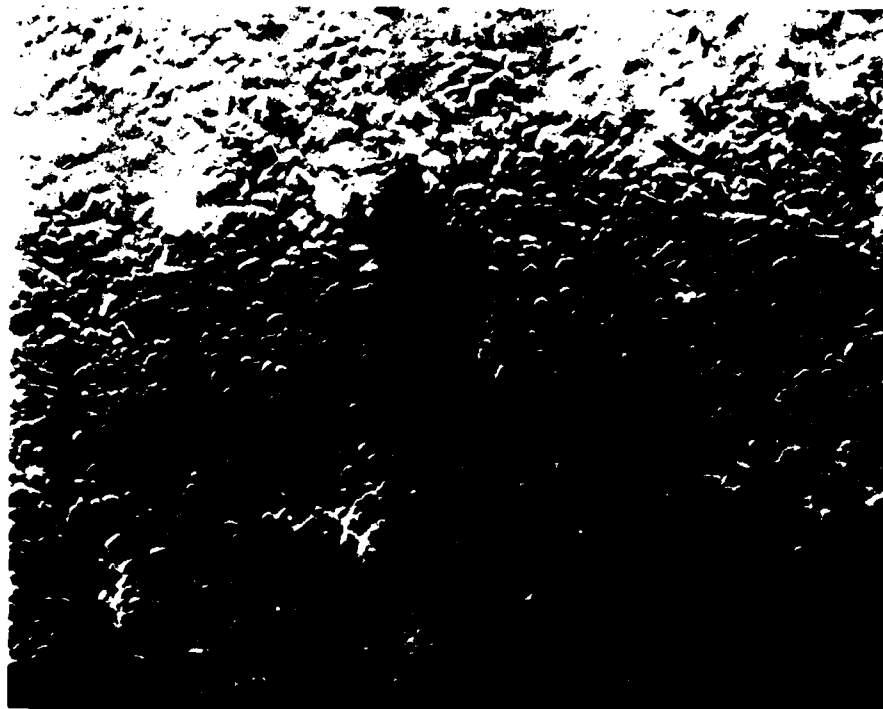
FIGURE 32 - Low Magnification SEM Micrograph showing the SiC Distribution in the
Vacuum Hot Pressed Commercial SiC/Al Composite.
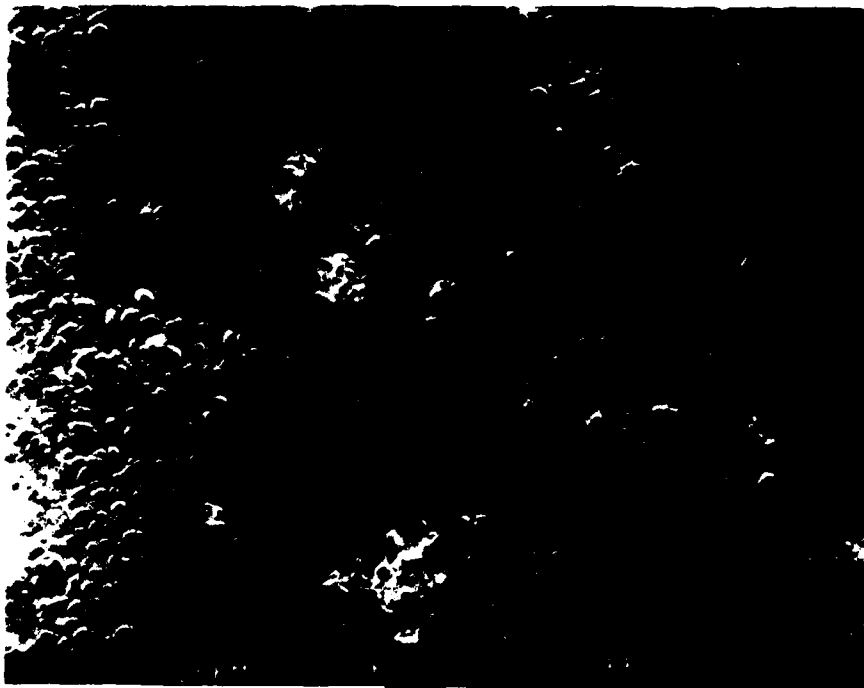
FIGURE 33 - Low Magnification SEM Micrograph showing the SiC Distribution in the Hot Isostatically Pressed Commercial SiC/Al Composite.

65
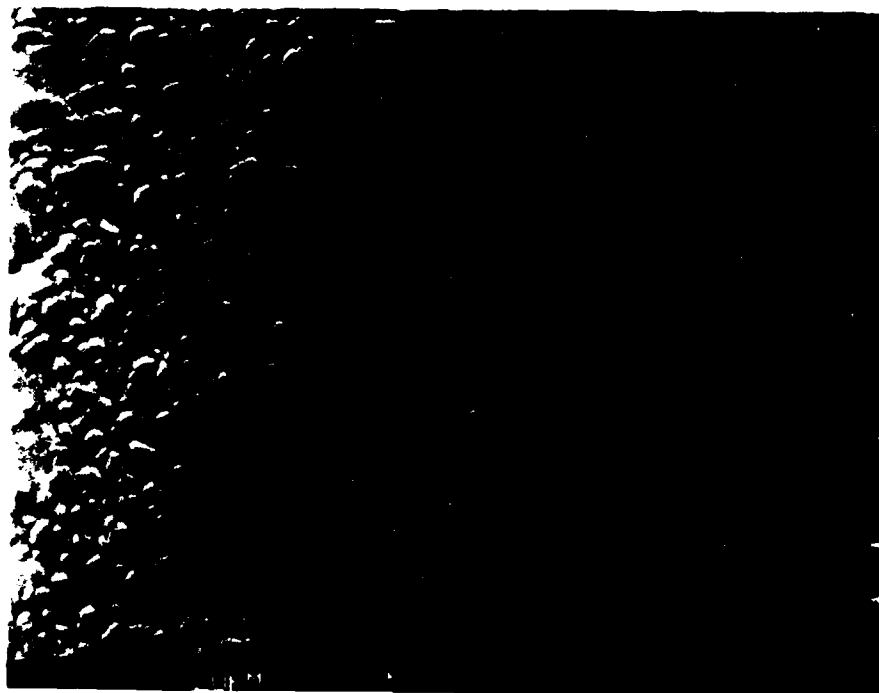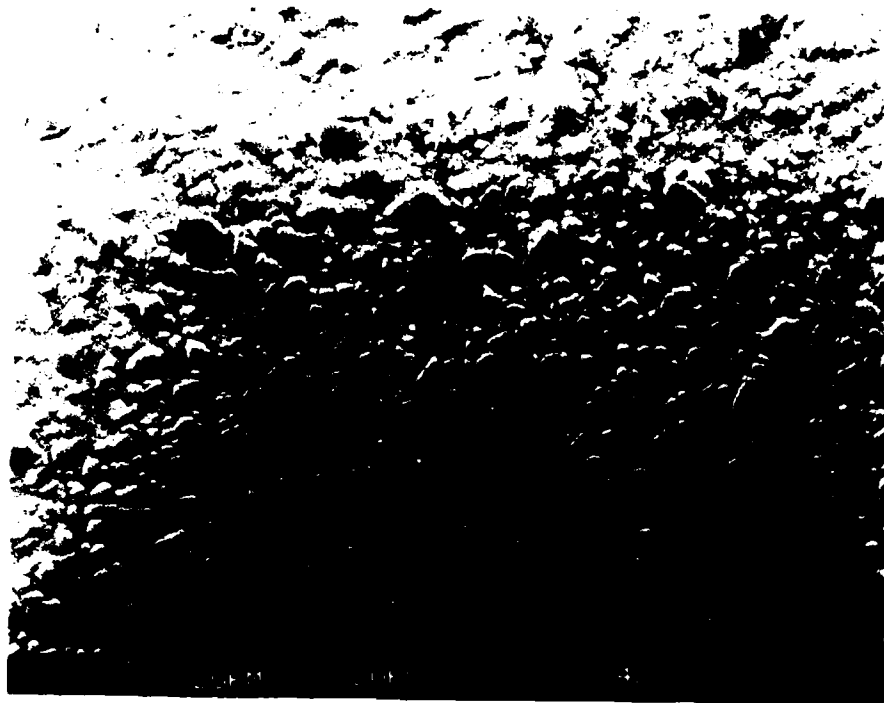
FIGURE 34 - Low Magnification SEM Micrograph Showing the SiC Distribution in the 5-30 Composite.

66

END

DATE

FILMD

3 – 88

DTIC